

# A multidisciplinary study of ecosystem evolution through early Pleistocene climate change from the marine Arda River section, Italy

Gaia Crippa<sup>a\*</sup>, Andrea Baucon<sup>b,c</sup>, Fabrizio Felletti<sup>a</sup>, Gianluca Raineri<sup>d</sup>, Daniele Scarponi<sup>e</sup>

<sup>a</sup>Università degli Studi di Milano, Dipartimento di Scienze della Terra “A. Desio,” via Mangiagalli 34, Milano, 20133, Italy

<sup>b</sup>Università di Modena, Dipartimento di Chimica e Scienze Geologiche, Via Campi 103, Modena, 41125, Italy

<sup>c</sup>Geology and Palaeontology Office, Geopark Naturtejo da Meseta Meridional – UNESCO Global Geopark. Municipality of Idanha-a-Nova – Centro Cultural Raiano. Av. Joaquim Morão, Idanha-a-Nova, 6060-101, Portugal

<sup>d</sup>Parco Regionale dello Stirone e del Piacenziano, Loc. Scipione Ponte 1, Salsomaggiore Terme, 43039, Italy

<sup>e</sup>Università di Bologna, Dipartimento di Scienze Biologiche, Geologiche e Ambientali, Via Zamboni 67, Bologna, 40126, Italy

(RECEIVED June 13, 2017; ACCEPTED November 22, 2017)

## Abstract

The Arda River marine succession (Italy) is an excellent site to apply an integrated approach to paleoenvironmental reconstructions, combining the results of sedimentology, body fossil paleontology, and ichnology to unravel the sedimentary evolution of a complex marine setting in the frame of early Pleistocene climate change and tectonic activity. The succession represents a subaqueous extension of a fluvial system, originated during phases of advance of fan deltas affected by high-density flows triggered by river floods, and overlain by continental conglomerates, indicating a relative sea level fall and the establishment of a continental environment. An overall regressive trend is observed through the section, from prodelta to delta front and intertidal settings. The hydrodynamic energy and the sedimentation rate are not constant through the section, but they are influenced by hyperpycnal flows, whose sediments were mainly supplied by an increase in Apennine uplift and erosion, especially after 1.80 Ma. The Arda section documents the same evolutionary history of coeval successions in the Paleo-Adriatic region, as well as the climatic changes of the early Pleistocene. The different approaches used complement quite well one another, giving strength and robustness to the obtained results.

**Keywords:** Early Pleistocene; Facies analysis; Body fossils; Trace fossils; Paleo-Adriatic

## INTRODUCTION

The complex interactions between organisms and their environments are an important aspect of the planet's evolution. Biotic and abiotic systems evolve in time and leave tracks in the biosedimentary record (e.g., Kowalewski et al., 2015; Wysocka et al., 2016; Martinelli et al., 2017; Scarponi et al., 2017a, 2017b). Unfolding such a record to pinpoint how ecosystems changed over time in response to paleoenvironmental modifications, however, requires a multidisciplinary approach including a well-established stratigraphic framework, a careful taxonomy, and a comprehensive ecological background (Dodd and Stanton, 1990). The basic data for paleoecology are adequately identified body fossils and trace fossils, which record the behavioral patterns of organisms through time, both correctly positioned within the stratigraphic framework. Though such a

multidisciplinary approach is widely recognized to be powerful in reconstructing paleoecosystems and their evolution, it is seldom implemented in the literature.

The lower Pleistocene marine succession of the Arda River (northern Apennines, Italy) represents an excellent site at which to apply multidisciplinary investigations (Crippa et al., 2016). The wealth of sedimentary structures and the excellent preservation of body and trace fossils make this marine succession a case study where we can integrate the abiotic and biotic components to resolve past ecosystems dynamics within a key time interval of climate change.

The early Pleistocene was characterized by climatic oscillations related to glacial/interglacial cycles, with the Mediterranean area being affected by these changes in both marine and continental settings (e.g., Bertini, 2010; Fusco, 2010; Scarponi et al., 2014; Combourieu-Nebout et al., 2015; Crippa et al., 2016; von Leesen et al., 2017). The most important biotic events recorded in the marine environment of the Mediterranean are the disappearance of taxa of subtropical affinity and the occurrence of “northern guests,” i.e., organisms presently living at higher latitudes in the

\*Corresponding author at: Università degli Studi di Milano, Dipartimento di Scienze della Terra “A. Desio,” via Mangiagalli 34, Milano, 20133, Italy. E-mail address: gaia.crippa@unimi.it (G.Crippa).

Northern Hemisphere, such as the bivalve *Arctica islandica*, the foraminifera *Hyalinea balthica*, and *Neogloboquadrina pachyderma* left-coiling, which migrated into the entire Mediterranean Sea through the Strait of Gibraltar during glacial periods since the Calabrian (early Pleistocene; Suess, 1883–1888; Raffi, 1986; Martínez-García et al., 2015). Recently, by analyzing the isotopic composition of the bivalve shells from the Arda River section, Crippa et al. (2016) observed that seawater temperature seasonality was the main variable of climate change within the study area during the early Pleistocene, in turn controlled by the Northern Hemisphere glaciation dynamics. In particular, strong seasonality and low winter paleotemperatures were assumed to be the main drivers for the widespread establishment of “northern guest” populations in the Paleo-Adriatic Sea.

Here, we pursue an integrated approach involving facies analyses and paleoecological observations to investigate the

relationships between body and trace fossils and their environment in the early Pleistocene of the Arda Section. The purpose of this paper is twofold: first, to compare the results of the analyses of sedimentology and body and trace fossils, evaluating to which extent these three different approaches complement one another and derive general implications for their combined use; and second, to reconstruct the paleoenvironmental evolution of the Arda River sedimentary succession based on the integration of three different tools and to interpret the succession taking into account the interplay between tectonic and climatic factors (both local and global).

## GEOLOGICAL SETTING

The Arda River section is located in northern Italy near the town of Castell'Arquato, at the margin of the northern Apennines facing the Po plain (Fig. 1). The northern

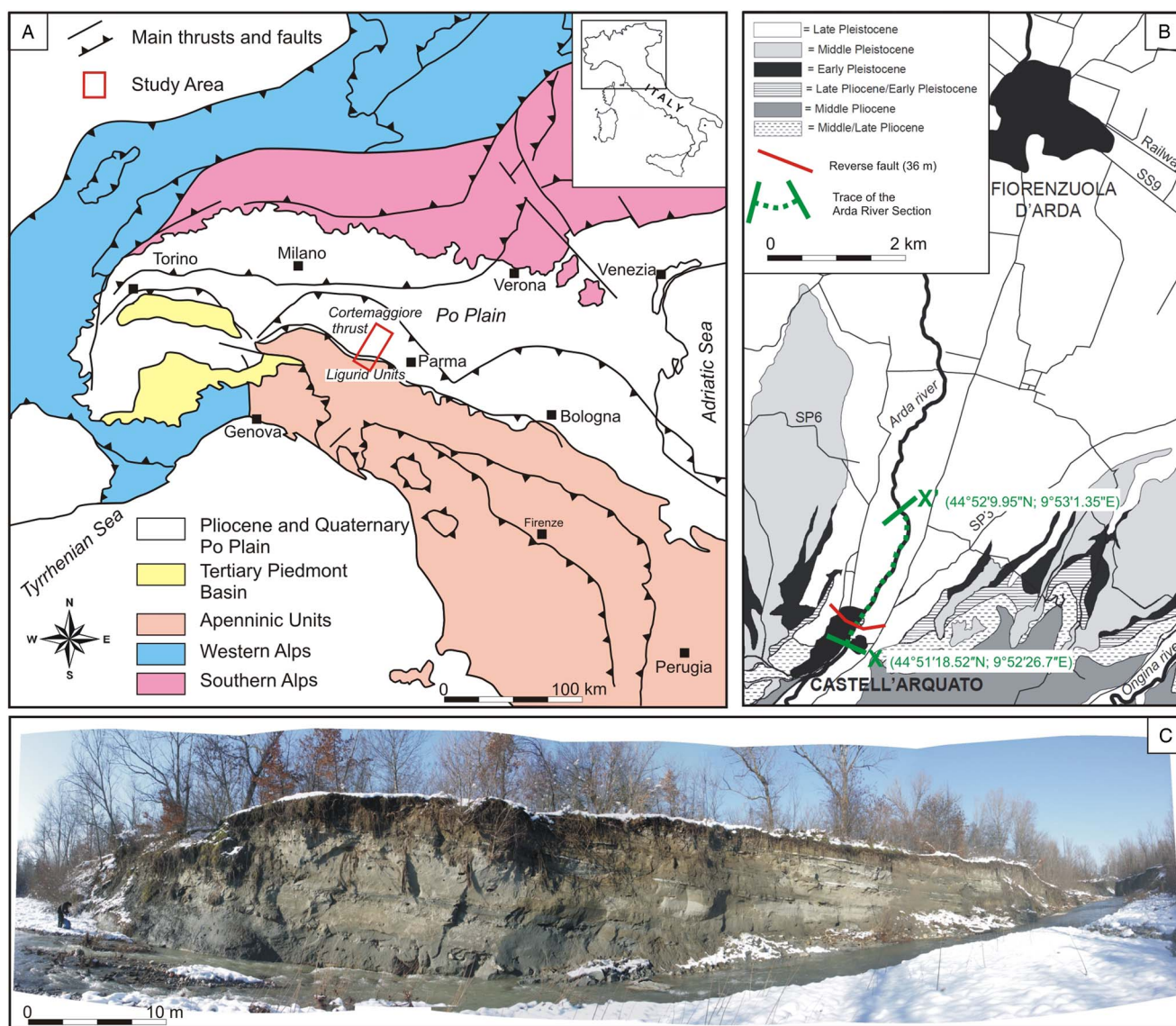


**Figure 1.** (color online) (A) Geological sketch map of northern Italy showing the study area (modified after Crippa et al., 2016). (B) Enlarged geological map of the Castell'Arquato basin with indication of the measured Arda River section (modified after Monesi et al., 2016). (C) Photograph of a part of the outcrop along the Arda River section (metric interval on the stratigraphic section; Fig. 2, 120–140 m).

Apennines are an orogenic wedge that started to form since the Oligocene as a result of the collision between the Corsica-Sardinia microplate and the Adria promontory, following the closure of the Mesozoic Ligurian-Piedmont Ocean (Carminati and Doglioni, 2012). Deformation migrated through time toward the east-northeast, gradually involving the Ligurid oceanic units and the Adria continental margin.

The Arda River section belongs to the Castell'Arquato basin, a small wedge-top basin developed since the Messinian (Miocene) at the eastern edge of the northern Apennine orogenic wedge as a result of the fragmentation of the Po Plain foredeep (Roveri and Taviani, 2003; Artoni et al., 2010; Fig. 1). It forms part of the northwestern extension of the Paleo-Adriatic Sea and is bounded to the north by the Cortemaggiore thrust and to the south by the emerged front of Ligurid units (Monegatti et al., 2001; Fig. 1A). The basin infill is characterized by several basin-wide, unconformity-bounded sedimentary cycles, recognized both on the outcrops and in the subsurface of the Po Plain and the central Adriatic Sea (Pieri, 1983; Ori et al., 1986; Ricci Lucchi, 1986). The Castell'Arquato basin is filled by a sedimentary succession of late Messinian (upper Miocene) to Holocene age, organized in a large-scale transgressive-regressive cycle controlled by tectonics, with beds forming a regular monocline dipping towards the north-northeast (Monegatti et al., 2001). The basal part of the filling succession comprises deep sea sediments postdating the Messinian salinity crisis (Ceregato et al., 2007; Calabrese and Di Dio, 2009), when marine conditions were restored in the Mediterranean Sea; upward, they pass into slope and shelf facies associations and then through a regressive trend to the middle Pleistocene continental alluvial deposits, which represent the final retreat of the sea in this area and the establishment of a continental environment with vertebrate faunas and freshwater mollusks (Cigala Fulgosi, 1976; Pelosio and Raffi, 1977; Ciangherotti et al., 1997). Detailed studies carried out in recent years through the integration of surface and subsurface data have resulted in a comprehensive stratigraphic and evolutionary model of the Castell'Arquato basin during the Pliocene and the early Pleistocene (Roveri et al., 1998; Monegatti et al., 2001; Roveri and Taviani, 2003). Insights into the paleogeography of the Po basin at the first major regression of the coastline, a consequence of the lowstand during the late early Pleistocene climate turnover (EPT), have been recently provided in figure 8 of Monesi et al. (2016).

The studied succession crops out along the Arda River and extends downstream of the bridge located at the entrance of the town of Castell'Arquato (northern Italy; Fig. 1B and C); the marine part, which is the subject of the present study, is 237m thick and bounded at the top (44°52'9.95"N, 9°53'1.35"E) by continental conglomerates (Fig. 2). The lowermost portion of the section is cut by a fault (Fig. 1B and 2), causing the repetition of the first 36m of the succession (base at 44°51'18.52"N, 9°52'26.7"E); the succession described here begins stratigraphically above the fault. The Arda River marine succession has a Calabrian

(early Pleistocene) age, ranging from ~1.8 to 1.2 Ma, based on magnetostratigraphy (Monesi et al., 2016) and calcareous nannofossil and foraminifera biostratigraphy, which allowed identification of three nannofossil (CNPL7, CNPL8, and CNPL9) and one foraminiferal (*Globigerina cariacensis*) biozones (Crippa et al., 2016).

## MATERIALS AND METHODS

### Sedimentology

The Arda River section has been measured bed-by-bed at 1 cm resolution. Bed thickness measurements were performed mainly with a Jacob's staff (e.g., a 1.5-m-high rod equipped with a clinometer and a flat sighting disc on top). The log was measured, recording the internal subdivisions of the individual beds or "depositional intervals" (i.e., depositional divisions or bed intervals in the sense of Ghibaudo [1992]). The thickness, grain size, presence of erosion surfaces, mud clasts, and structure of every internal division of the beds were recorded separately for each bed in addition to the total bed thickness. The grain size was measured using a grain-size comparator chart. In order to account for amalgamation of beds, partially amalgamated beds were measured as individual layers. This was possible through detecting the subtle grain-size breaks that are associated with amalgamation surfaces. To make the measurement of the section reproducible and available also for other analyses, labeled nails were fixed every meter from the base to the top of the section, according to the attitude of the bedding.

### Body fossils

Fossils were collected bed by bed, from a total of 144 beds over the entire studied section; for each of the targeted beds, two rectangles (50 cm wide and 10 cm tall) were delimited and all exposed fossils sampled. Fossil specimens (mainly mollusks) were then washed and cleaned from the encasing sediment using an air drill, in the case of hard sediment, or a scalpel, in the case of soft sediment, and a unique ID was assigned to each of them; they were identified at generic and/or specific level (where feasible) based on relevant literature (e.g., Williams et al., 2000, 2006; Ceregato et al., 2007; Crippa and Raineri, 2015) and subsequently counted (see Supplementary Information A1 for a detailed explanation). In addition, to aid environmental interpretation of fossil assemblages, it was observed if the specimens (bivalves and brachiopods) were articulated or disarticulated and each specimen retrieved was carefully inspected, looking for the presence of the following taphonomic features: (1) roundness vs. sharpness of fragments; (2) corrosion, due to the combined effect of abrasion and dissolution (Brett and Baird, 1986); (3) external and/or internal bioerosion, produced by predators, necrophages, or the presence of domicinia; (4) internal and/or external encrustations caused by episkeletobionts (sensu Taylor and Wilson, 2003); (5) ornamentation, which is usually fragile and can be lost during



post-mortem processes; and (6) original color and pattern of the shell/fragment surface (Supplementary Information A2 and Supplementary Table A1). Based on the analysis of these features, we identified the associations defined by Brenchley and Harper (1998): (1) life assemblages, (2) neighborhood assemblages, and (3) transported assemblages.

A qualitative paleoecological analysis was then performed, in which the assemblages of the Arda River section were tentatively compared to the recent Mediterranean biocenoses. As the majority of the retrieved taxa is represented by living species, the fossil associations recovered were grouped in biofacies and attributed to the present day depositional environments based on the occurrence of characteristic taxa described by Pérès and Picard (1964). The abbreviation used are: SFBC, biocenosis of fine-grained well sorted sands; SFS, biocenosis of shallow water fine-grained sands; DC, biocenosis of coastal detritic bottoms; and VTC, biocenosis of terrigenous mud.

### Trace fossils

Sedimentology and body fossil paleontology have been integrated with ichnological analysis, using the workflow for integrated facies analysis (McIlroy, 2008). Because of the predominantly vertical outcrops and the high bioturbation intensity, the ichnofabric approach has been used. The ichnofabric analysis method considers the overall texture of a bioturbated sediment and, as such, it is the ichnological equivalent of facies analysis (Taylor et al., 2003; McIlroy, 2004, 2008).

Data collection consisted of recording the ichnofabric attributes of the Arda River section in the field at regularly spaced intervals (“samples”). Each of the studied samples was approximately 25 cm thick and the spacing between successive samples was 1 m. The recorded ichnofabric attributes are: (1) primary sedimentology (Taylor et al., 2003); (2) degree of bioturbation, quantified by the ichnofabric index (ii) methodology (Bottjer and Droser, 1991); and (3) components of the ichnofabric, including either distinct trace fossils or biodeformational structures with indistinct outlines (Schäfer, 1956; Wetzel and Uchman, 1998; Taylor et al., 2003). Relative abundance, burrow size, tiering, trace fossil frequency, and distribution at the sample scale have also been observed (Bromley, 1996; Taylor et al., 2003; Gingras et al., 2011).

Visual analysis of each sample included observation of (1) the weathered surface of the outcrop; (2) the fresh surface of the outcrop, exposed with a trowel (a minimum of three fresh surfaces of about 25 × 25 cm have been observed); and (3) the enhanced fresh surface, obtained by dropping water on the fresh surface to enhance color contrast and to differentiate weathered traces from the surrounding sediment.

Each sample has been attributed to an ichnofabric class that has been distinguished on the basis of the degree of bioturbation, bioturbation distribution (Gingras et al., 2011), diversity (i.e., the number of ichnotaxa present; Bromley, 1996), and components of the ichnofabric.

## RESULTS AND INTERPRETATIONS

### Facies analysis

Facies analysis was carried out on marine sediments deposited during phases of advance of fan deltas when Apennine tectonic uplift renewed sediment dispersal and provided the basin with a steeper margin. Following the genetic classification scheme proposed by Zavala et al. (2011) for flood-generated delta-front lobes, the deposits of the Arda section (Fig. 2) have been grouped in three main facies categories related to the three main processes that characterize sustained hyperpycnal discharges (i.e., hyperpycnal flows; Mutti et al., 2000; Tinterri, 2007) in marine settings: (1) bed load (Facies B: bed-load related sedimentary facies); (2) turbulent suspension (Facies S: suspended-load-related sedimentary facies); and (3) lofting (Facies L: lofting-related sedimentary facies). Facies codes and relative descriptions are shown in Table 1.

#### *Facies related to bed-load processes (Facies category B)*

Facies category B (Fig. 3) is composed of massive (GmE; Fig. 3A) and cross-stratified (or crudely stratified) conglomerates (Gp; Fig. 3D) with abundant coarse- to fine-grained sandstone matrix (matrix supported). Large clasts in this facies appear to float in a medium- to coarse-grained sandstone matrix. Individual sets of cross bedding commonly show thicknesses between 0.1 and 0.5 m. The foreset inclination in general does not exceed 15°. Bounding surfaces between bedsets can be erosional. Lag deposits (Lag; Fig. 3E and F) represented by gravel carpets with bioclastic and sandy (very coarse) matrix are frequent. This facies category also includes mud clast-supported conglomerate (GmM; clay-chips; Fig. 3A–C). Mudstone intraclast diameter ranges from 0.5 to 20 cm and their shapes range accordingly from rounded sub-spherical to rounded tabular.

*Interpretation.* This facies category includes different coarse-grained deposits related to shear/drag forces exerted by the overpassing long-lived turbulent (hyperpycnal) flow over coarse-grained materials lying on the flow bottom (Fig. 3). High-density flows triggered by river floods can mix and deposit skeletal remains from different shallow-water communities. Regardless, accumulations of shells are rare features in this bed-load related sedimentary facies.

#### *Facies related to the collapse of suspended load (facies category S)*

Facies category S (Fig. 4) are mostly fine-grained sandstone strata ranging from lamina-sets a few millimeters thick, to beds and bedsets several tens of decimeters thick, with massive stratification (Sm; Fig. 3E and F); horizontal (Sh; Fig. 4A and D) or hummocky cross stratification (HCS; Fig. 4E); tabular and oblique cross stratification (Sp, Sx; Fig. 4B); and small-scale cross lamination (Sr, St; Fig. 4A and C). Many beds are sharp-based and fine upward,



**Table 1.** Facies classification scheme utilized for the Arda section following the genetic classification proposed by Zavala et al. (2011). All these facies categories are genetically related and occupy a definite position within the hyperpycnal system. The B facies is diagnostic of proximal areas and progressively disappears as the flow enters the area of lobe deposition. The S facies is the consequence of the loss of flow capacity and is typical of the medium to distal parts of the system. The L facies results from the flow inversion, which is diagnostic of flow-margin areas (both down the depositional axis and laterally along the axis).

Facies categories	Code	Facies	Sedimentary features
<i>Facies B</i> ( <i>bed-load related</i> )	<i>GmE</i>	<i>Massive grain-supported gravels</i>	Massive, grain supported polygenic gravels. Beds have an erosive base and are usually heavily cemented (Fig. 3 A).
	<i>GmM</i>	<i>Massive mud clasts deposits</i>	Massive rip-up clasts deposits. Sandy matrix with abundant bioclasts (bivalves and gastropod shell fragments). Beds have an erosive base. Mud clasts are ripped from muddy layers (Fig. 3 A, B, D; Fig. 4 E; Fig. 5 C).
	<i>Gp</i>	<i>Planar stratified gravels</i>	Gravels with horizontal or oblique planar stratification. Clasts are usually embriacated. Some of these beds are heavily cemented (Fig. 3 D).
	<i>Lag</i>	<i>Lag deposits</i>	Gravel carpets with bioclastic and sandy (very coarse) matrix (Fig. 3 E).
<i>Facies S</i> ( <i>suspended-load-related</i> )	<i>Sp</i>	<i>Planar oblique stratified sands</i>	Mostly bioclastic, planar oblique stratified coarse grained sands. Beds are heavily cemented and bioturbated. Bioturbation is in the form of vertical tunnels (Fig. 4 B, F).
	<i>Sx</i>	<i>Planar cross stratified sands</i>	Fine to medium grained planar cross stratified sands. Bioturbation is apparently absent. (Fig. 5C).
	<i>HCS</i>	<i>Hummocky cross stratified sands</i>	Fine to coarse grained hummocky stratified sands. Beds are usually rich in bioclasts. Bioturbation is apparently absent. Occurrence of wood fragments and logs. (Fig. 4 E).
	<i>St</i>	<i>Trough cross stratified sands</i>	Fine to coarse grained trough cross stratified sands. Beds are usually rich in bioclasts. Bioturbation is apparently absent. Occurrence of wood fragments and logs (Fig. 3 C, B).
	<i>Sr</i>	<i>Ripple cross stratified sands</i>	Fine grained sands with wave or current ripples, sometimes with well-developed climbing ripples laminasets(current). No evidence of bioturbation (Fig. 4 A, B, D; Fig. 5 A, C).
	<i>Sh</i>	<i>Horizontally stratified sands and silts</i>	Horizontally stratified fine and very fine grained sands and silts usually rich in organic matter (small wood fragments) and mollusk fragments (Fig. 3 A, C, D; Fig. 4 A, D, F; Fig. 5 B, C, D).
	<i>Sm</i>	<i>Massive sands</i>	Very fine to medium grained massive sands. Beds are locally bioturbated (Fig. 3 A, E, F; Fig. 4 F; Fig. 5 C).
	<i>HeB</i>	<i>Heterolitic bedding</i>	Heterolitic fine grained sands to mud. Flaser, wavy and lenticular bedding.
<i>Facies L</i> ( <i>lofting-related</i> )	<i>Fm</i>	<i>Massive fines</i>	Structureless silts and muds with minor very fine sands. Beds are locally heavily bioturbated. Presence of in-life position marine bivalves in the lower part of the stratigraphic section. In the upper part (continental deposits) frequent root systems and vertebrates (Fig. 5 A, B, E, F).
	<i>CCB</i>	<i>Carbonatic Cemented Beds</i>	Cemented levels, rich in carbonate. (Fig. 5 B)

Bedset-bounding surfaces can be erosional (Fig. 5C). Above follow sandstones that are either massive or with horizontal, hummocky, tabular, or oblique cross stratification (Sp, Sx, HCS, St, Sr, Sh, or Sm; Table 1). Sharp-based, normally graded, tabular to lenticular lags of concave-down shells may occur at the base of the strata. Carbonaceous remains and wood fragments are also common within massive sands. Flasers, wavy and lenticular bedding (Heb; Table 1), from a few millimeters to several centimeters thick, are often intercalated with these sandstones. Finally, above the sandstones follow massive to laminated siltstones and mudstones

arranged in thin couplets (Fm; Table 1), ranging in thickness from a few mm up to 1 m and accumulated by normal settling when the flow completely stopped.

Each cycle shows a complicated internal arrangement. The vertical and lateral facies anisotropy and the relatively rapid accumulation result in the common occurrence of water-escape features such as load cast and flame structures (Fig. 5D). Field observations suggest a close association of this facies with channel fill deposits.

A biocalcarenite body occurs (Fig. 5E and F) 45 m from the base of the succession. It forms basinward-prograding wedges



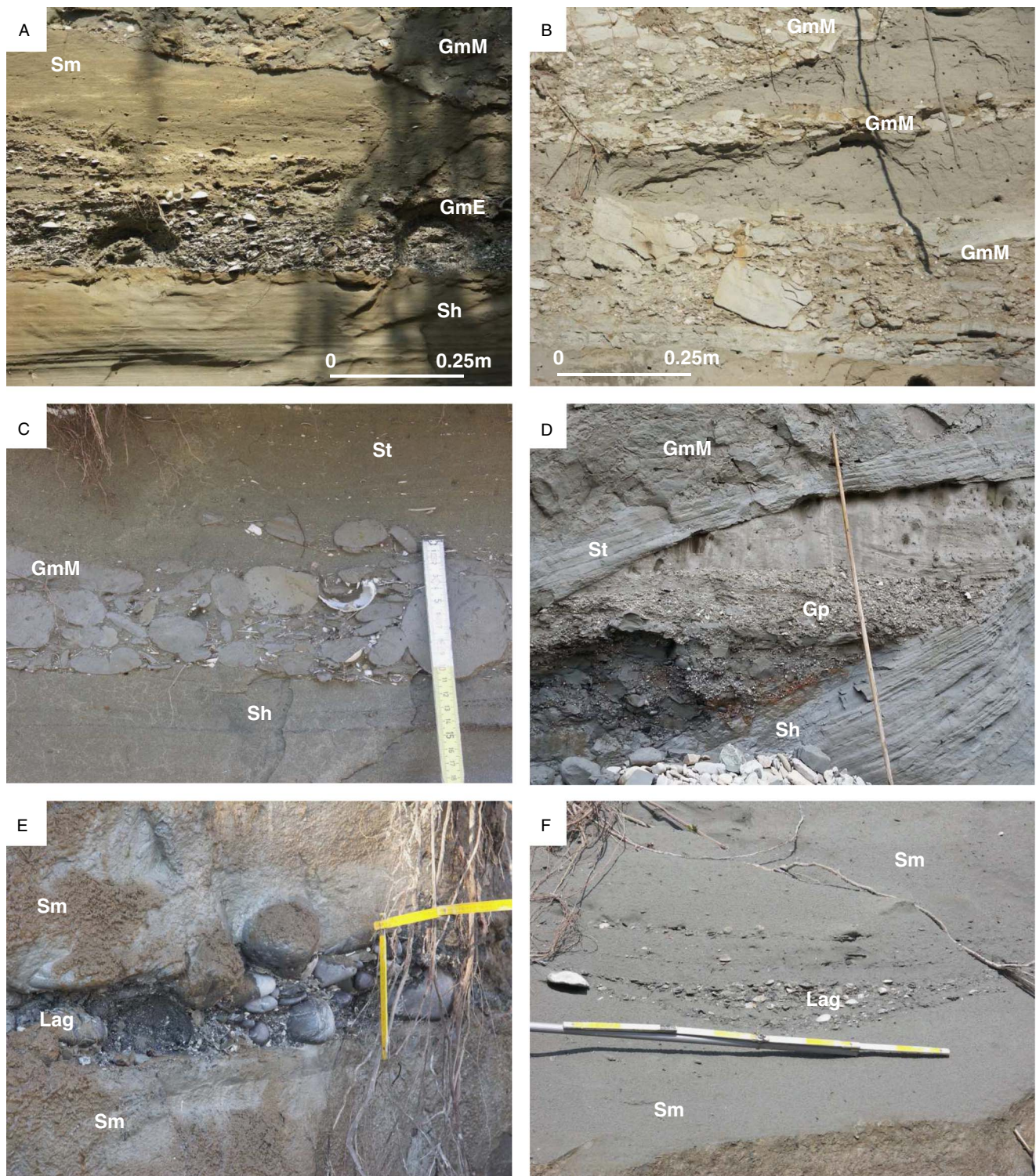


**Figure 3.** (color online) (A–F) Facies related to bed-load processes (Facies B). This category includes different coarse-grained deposits related to shear/drag forces exerted by the overpassing long-lived turbulent (hyperpycnal) flow over coarse-grained material lying on the flow bottom. See Table 1 for facies codes and relative description. Corresponding metric intervals on the stratigraphic section (Fig.2): (A) 179.10 m; (B) 114 m; (C) 94.10 m; (D) 28.20 m; (E) 224.80 m; and (F) 131.90 m.

composed of alternating well- or poorly cemented layers with dense accumulations of reworked shells. It typically displays a tripartite geometry, whose topset horizontal strata are intensely bioturbated, and may contain abundant articulated bivalves and

fragmented calcareous algae, while foresets and bottomsets are characterized by dense accumulations of reworked shells.

From 130 to 132 m, very fine-grained limestones form lenticular or pinching and swelling beds up to 0.25 m thick



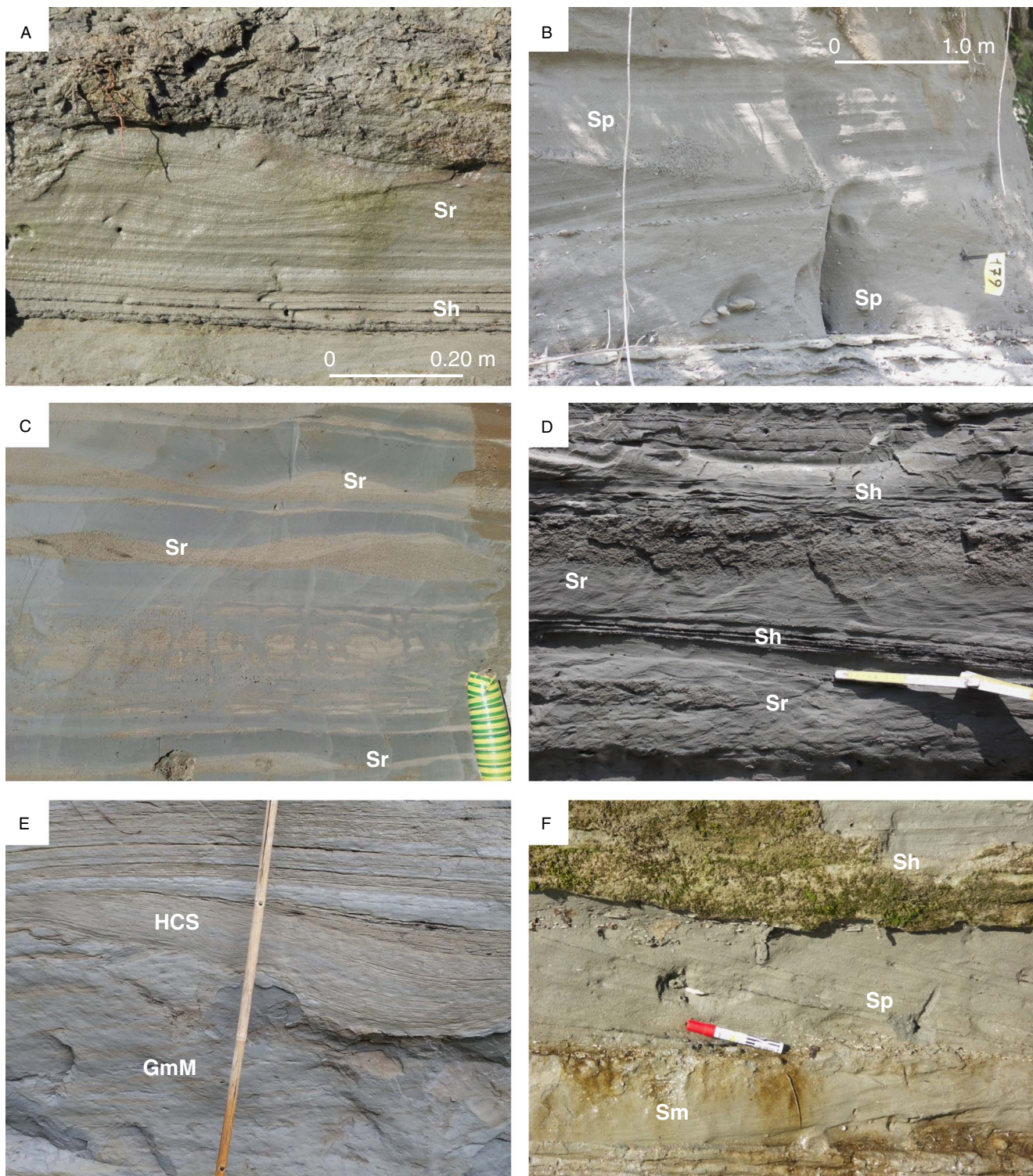


**Figure 4.** (color online) (A–F) Facies related to the collapse of suspended load (Facies S). This category mostly includes fine-grained sediments transported as suspended load, forming thick and commonly complex intervals that can be massive or display traction plus fallout sedimentary structures. See Table 1 for facies codes and relative description. Corresponding metric intervals on the stratigraphic section (Fig. 2): (A) 177.20 m; (B) 134 m; (C) 193.80 m; (D) 230.60 m; (E) 184.60 m; and (F) 194.20 m.

(Fig. 5B). The beds have sharp bases and tops and may be laminated. The thin section analysis reveals that these beds are predominately composed of a fine-grained calcareous matrix including calcareous microspheroids and organic matter.

From 217 to 237 m, the sequence is characterized by coarse-grained sands and pebbly sandstones with low-angle cross-stratification (Sx, Sh, St, Sm, HCS, and Heb; Table 1). Large clasts appear floating in a medium- to



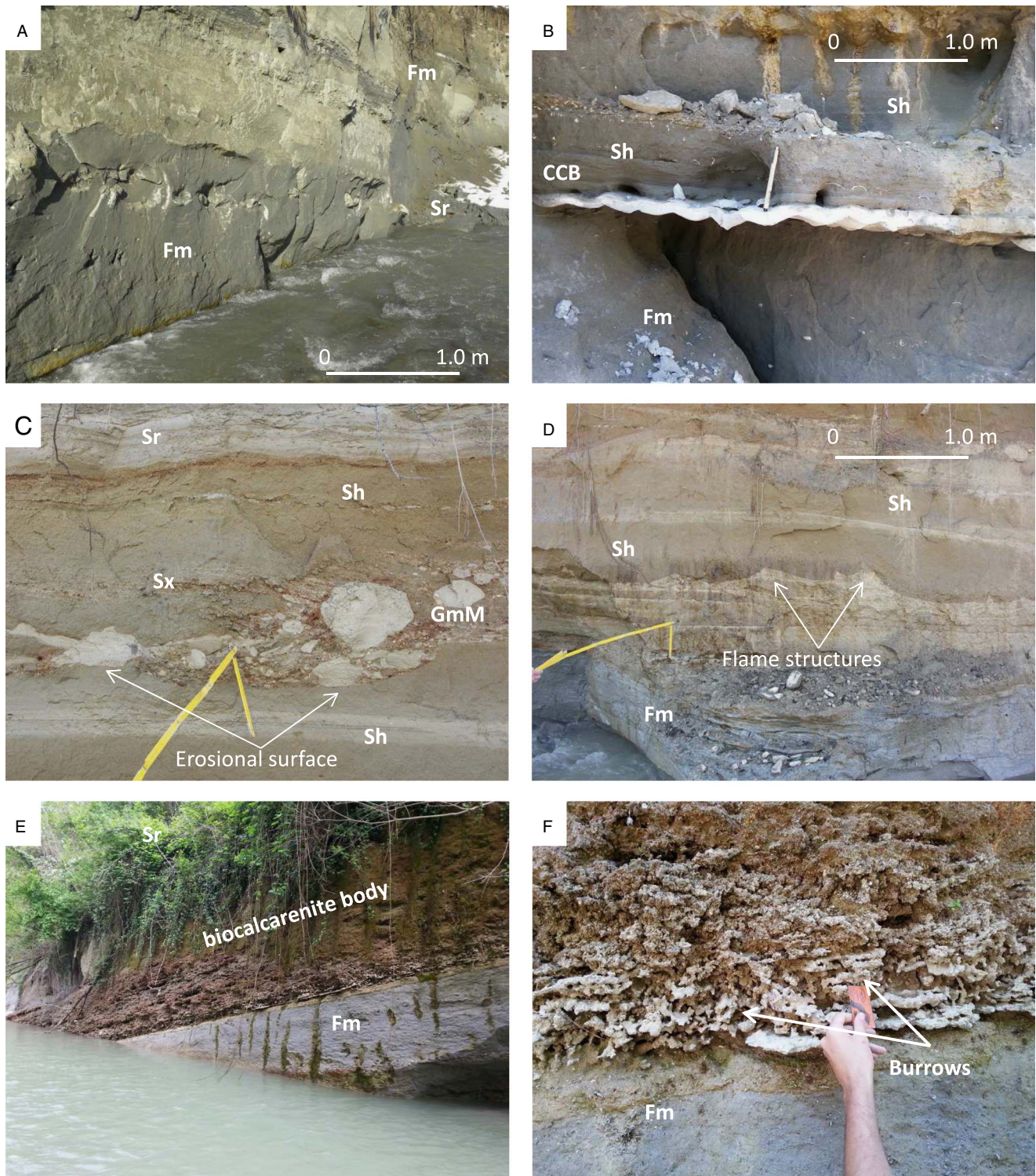


**Figure 5.** (color online) (A) Facies related to flow lofting (Facies L). It is characterized by thin couplets of massive to laminated siltstones and mudstones (Fm), transported by the hyperpycnal flow, which accumulated by normal settling when the flow completely stopped (107.40 m). (B) Cemented levels, rich in carbonate (CCB; 130.20 m). See Table 1 for facies codes and relative description. (C) Erosional bedset-bounding surfaces (114 m). (D) Rapid accumulation results in the common occurrence of water-escape features such as load cast and flame structures (184.60 m). (E and F) Biocalcarenic body (46 m). It forms prograding wedges typically displaying intense bioturbation. Foresets and bottomsets are characterized by dense accumulations of reworked shells.

coarse-grained sandstone matrix. Individual sets of crossbeds (Sx, St) commonly show thicknesses between 0.3 and 1 m and asymptotic relationships with top and base. The

foreset inclinations do not usually exceed 20°. This facies association is attributed to littoral (transitional) environments.



From 237 to 300 m, the sequence comprises continental sediments arranged in four main cycles, each characterized by massive or crudely stratified, partially cemented, fluvial gravel beds from 1 to 4 m thick (GmE, Gp; Fig. 2, Table 1), passing rapidly upward to sands, silts, and muds packed in beds from few meters up to 15 m thick. In situ root systems and tree trunks, together with CaCO<sub>3</sub> nodules and typical terrestrial gastropods (e.g., *Pomatias elegans*, *Carychium tridentatum*, and *Retinella* [*Retinella*] *olivetorum*) are abundant in fine-grained beds, suggesting continental swamp environments.

**Interpretation.** Deposits of the Arda section display a complicated vertical arrangement of different lithofacies reflecting cyclic depositional changes between suspended-load and bed-load-dominated facies associated with different velocity and fallout rates. These cyclical and gradual changes between different facies are the result of near-continuous deposition from a quasi-steady turbulent flow (Zavala et al., 2011). Distinctive features observed in the studied deposits are: (1) the sharp based and normally graded beds containing HCS; (2) gradual and sharp facies transitions without a definite and predictable internal arrangement; (3) the abundant rip-up mudstone clasts and shells; (4) internal and laterally discontinuous erosional surfaces; (5) scarce burrows; and (6) a basal coarsening-upward interval (Mutti et al., 2000; Zavala et al., 2006, 2011). The studied deposits evolve laterally into packages of lofting rhythmites. These features are most likely related to bed-load processes developed at the base of a hyperpycnal flow (i.e., long-lived turbulent flow) and tend to dominate the proximal to medial parts of a river-delta system.

The biocalcarenic body occurring 45 m from the base of the succession shows an internal geometry suggesting that biocalcarenic deposits are formed during periods of decreased input of fine-grained terrigenous sediments (or sediment starved conditions) whose fossiliferous content indicates high-energy levels in the shelf environments. Different physical conditions can be assumed for their formation, such as reduced terrigenous input or strong bottom reworking by currents. Massari and Chiocci (2006) describe the formation of very similar Pliocene-Quaternary basinward-prograding biocalcarenic wedges (detached from the shore and below the storm-wave base) along the submerged margins of the Mediterranean area by means of processes of sediment reworking from a nearshore by pass zone and of storm-driven down-welling flow. The cyclical nature of these biocalcarenites, observed in the Castell'Arquato basin (Stirone section, Cau et al., 2013, 2017), has been hypothesized to be orbitally controlled by obliquity and/or precession cyclicity.

According to Mutti et al. (2003), the Arda River succession can be interpreted as a flood-dominated, fan-delta system accumulated in roughly tabular lobes extending from alluvial conglomerates to shelfal siltstone and mudstone. The associate deposits (hyperpycnites; Mulder et al., 2003) are closely related to direct fluvial discharge. Observed facies associations clearly show as flood-generated dense flows enter seawaters as catastrophic and inertia-dominated

relatively unconfined flows. Coarser materials tend to accumulate at the front of the flow, giving way to a horizontally negative grain-size gradient. Sedimentation occurs mainly in a mouth bar (characterized by sigmoidal bedding) and in associated flood-generated delta-front sandstone lobes.

This study suggests that the Arda River succession corresponds to the subaqueous extension of a fluvial system. It originated when the river in flood directly discharged a sustained (Carruba et al., 2004; Felletti et al., 2009) and relatively denser turbulent mixture of fresh water and sediments (hyperpycnal flows; Bates, 1953) into the receiving standing body of water. This system extended for kilometers away from the river mouth and developed a predictable path of genetically related facies (Browne and Naish, 2003; Mancini et al., 2013; Marini et al., 2013; Milli et al., 2016; Bruno et al., 2017) during its travel basinward.

## Body Fossils

The fossil associations of the Arda River succession contain a very diversified fauna composed mainly of several species of bivalves and gastropods; brachiopods, corals, serpulids, echinoderms, scaphopods, and barnacles also occur. The associations have been grouped into 11 biofacies, based on the presence of key species, taphonomic evaluation (Supplementary Information A2 and Supplementary Table A1), and (paleo)ecology of the fossils recovered (Fig. 6A–F, 7A–F, 8A–N).

### Biofacies 1

This biofacies occurs in fine-grained massive siltstones and sandstones (Facies L) at the base of the section (37.05–43.25 m). It is composed mainly of seminafaunal/infaunal organisms and by cemented/byssate epifaunal taxa; many rheophilous taxa (e.g., *Astarte fusca*, *Glycymeris inflata*, *Glycymeris glycymeris*, and *Clausinella fasciata*) are present (Fig. 6A, 8A, C, D). The taphonomic preservation is generally good (Supplementary Information A2 and Supplementary Table A1).

**Interpretation.** The occurrence of disarticulated rheophilous shelf related taxa indicates neighborhood assemblages of a high-energy environment winnowed by currents in an offshore transition setting. The negligible presence of shoreface key taxa (*Chamelea gallina*, *Spisula subtruncata*, and *Acanthocardia tuberculata*) showing high taphonomic degradation suggests a transport from shallower settings.

### Biofacies 2

This biofacies occurs in fine-grained massive silty to muddy lithologies (Facies L) below and above the biocalcarenic body (44.90 m; 47.35–49 m; 56.35–58.35 m); it is mainly represented by few specimens of seminafaunal/infaunal species typical of muddy-detritic and muddy shelf substrates (e.g., *Venus nux*, *Turritella tricarinata pliorens*, *Naticarius stercusmuscarum*, and *Pelecypora brocchii*), showing excellent preservation (Fig. 6C, D 8E, F, Supplementary Information A2



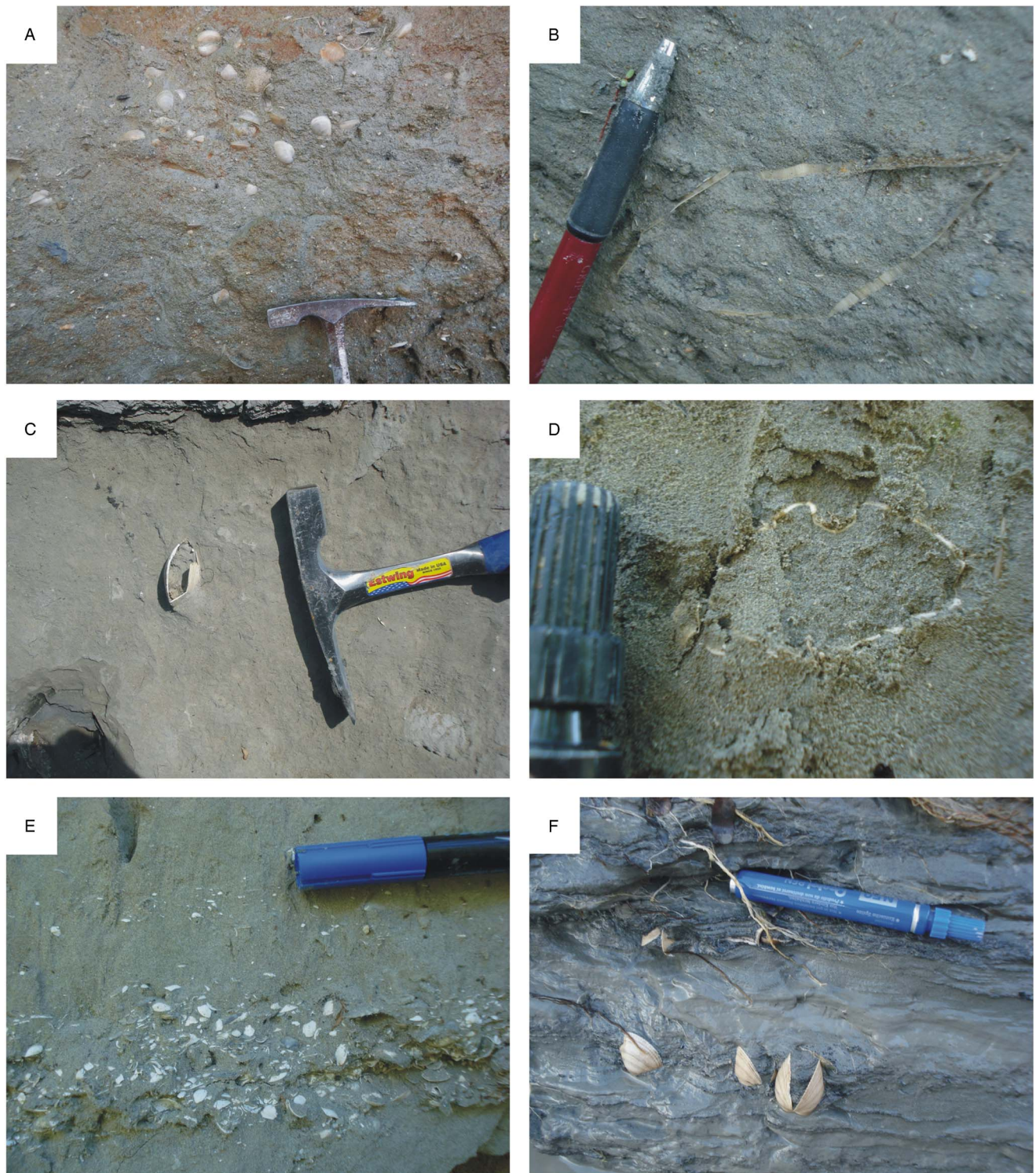


**Figure 6.** (color online) Fossiliferous beds of the Arda succession. (A) Articulated specimens of *Glycymeris inflata* (42 m, Biofacies 1, Cycle 0). (B) Section of an articulated specimen of *Pinna* sp. (54.20 m, Biofacies 10, Cycle I). (C) Articulated specimen of *Pelecyora brocchii* in life position (57.35 m, Biofacies 2, Cycle I). (D) Echinoid specimen (58.35 m, Biofacies 2, Cycle I). (E) Shell accumulation mainly containing specimens of *Spisula subtruncata* (68.53 m, Biofacies 4, Cycle I). (F) Life assemblage of articulated specimens of *Glycymeris insubrica* (133.90 m, Biofacies 9, Cycle IV).



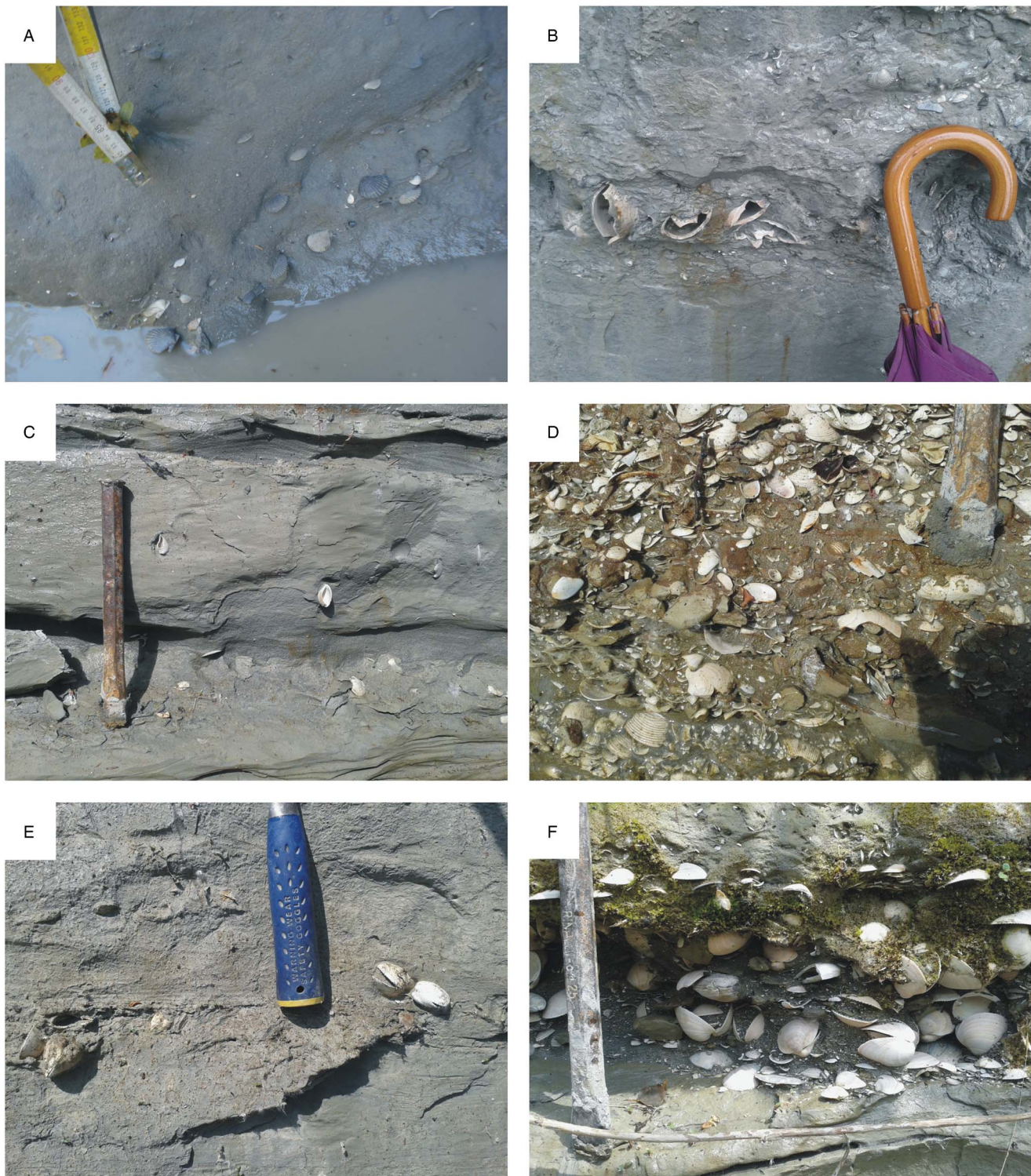


**Figure 7.** (color online) Fossiliferous beds of the Arda succession. (A) Bed with several specimens of *Aequipecten opercularis* (134.35 m, Biofacies 9, Cycle IV). (B) Articulated specimen of *Arctica islandica* in life position and lacking internal sediment filling (224.30 m, Biofacies 6, Cycle VII). (C) Specimens of *Chamelea gallina* with empty valves in life position (234 m, Biofacies 5, Cycle VI). (D) Accumulation bed with mainly disarticulated bivalves (234.40 m, Biofacies 5, Cycle VII). (E) Articulated specimens of *Glycymeris insubrica* (235.70 m, Biofacies 5, Cycle VII). (F) Accumulation bed with articulated specimens of *Glycymeris insubrica*, representing the most abundant species at the top of the section (236.80 m, Biofacies 5, Cycle VII).



and Supplementary Table A1). Corals, echinoids, brachiopods, and non-rheophilous mollusks are also present.

*Interpretation.* The sparse presence of *V. nux* and *P. brocchii* along with echinoids, brachiopods, and corals suggest a low-energy lower offshore transition setting characterized by normal marine salinity and oxygen conditions.

### Biofacies 3

This biofacies occurs in biocalcarenite (45.65–46.05 m; Facies S) and is represented by sparse and poorly preserved valves of epifaunal mollusks: *Aequipecten opercularis*, *Aequipecten scabrella*, and *Ostrea edulis* (Supplementary Information A2 and Supplementary Table A1).

*Interpretation.* The sparse mollusk content associated with poor taphonomic preservation within coarse-grained deposits allows only a generic interpretation of a transported assemblage from relatively high-energy settings.

### Biofacies 4

This biofacies occurs in fine-grained massive siltstones (59–70.02 m; 106.50–111.60 m; Facies L). Several key infaunal, shoreface to offshore transition, well-preserved taxa typical of muddy sands are found, specifically *Glycymeris insubrica*, *A. tuberculata*, *C. gallina*, *S. subtruncata*, and *Neverita josephinia* (Fig. 6E, 8E, F; Supplementary Information A2 and Supplementary Table A1).

*Interpretation.* The ecological and taphonomic signatures of this biofacies suggest life and neighborhood assemblages of shallow marine, high-energy offshore transition environments (Facies L); the faunal composition can be compared to the recent Mediterranean biocenosis of SFBC (Pérès and Picard, 1964).

### Biofacies 5

This biofacies occurs in an alternation of fine-grained sandy to silty and muddy lithologies (217.90–223.20 m; 230.80–237 m; Facies S and B). It contains mainly semi-infaunal/infaunal taxa living in shallow water muddy sands (e.g., *G. insubrica*, *A. tuberculata*, *C. gallina*, *Ensis ensis*, *Loripes orbiculatus*, *Cylichna cylindracea*, *Atlantella pulchella*, and *N. josephinia*), together with species of upper shoreface (*Donax* spp.) and of wave-protected environments (*Lucinella divaricate*; Fig. 7C–F; 8L). Toward the top, *G. insubrica* becomes the most abundant species (Fig. 7E and F), with numerous articulated specimens found in life position in muddy beds; trunks and plant remains are also found. All the specimens are well preserved (Supplementary Information A2 and Supplementary Table A1).

*Interpretation.* Biofacies 5 indicates life and neighborhood assemblages of upper shoreface setting, due to the presence of key taxa *Ensis ensis* and *Donax* spp.; the faunal composition is comparable to the SFBC and SFS biocenoses of the recent Mediterranean Sea (Pérès and Picard, 1964). Semi-infaunal/infaunal taxa are dominant,

suggesting a high-energy shallow water environment, which may prevent the colonization by epifaunal species; the presence of species living in wave-protected environments, however, suggests a more heterogeneous substrate with quieter areas. In addition, toward the top of the section, the disappearance of stenohaline species and the increase of euryhaline taxa, suggests settings affected by river discharge. Indeed, *G. insubrica*, which can also thrive in low salinity settings (e.g., Malatesta, 1974; Raineri, 2007; Crmčević et al., 2013), becomes the dominant species in the upper part of the section. Biofacies 5 differs from Biofacies 4 by the presence of shallower water taxa (e.g., *Donax* spp.), which are absent in Biofacies 4.

### Biofacies 6

This biofacies is found in fine-grained massive clayey horizon (224.20–224.30 m; Facies L), hosting several articulated specimens of *Arctica islandica* in life position and lacking sediment filling inside the valves (Fig. 7B), associated with the shallow water *S. subtruncata*, (average preferred depth = 6.60 m, standard deviation = 7.3 m; Wittmer et al., 2014) both showing an excellent preservation (Supplementary Information A2 and Supplementary Table A1).

*Interpretation.* The co-occurrence of lower shoreface *S. subtruncata* and of the “northern guest” *A. islandica* suggests a lower shoreface/offshore transition setting.

### Biofacies 7

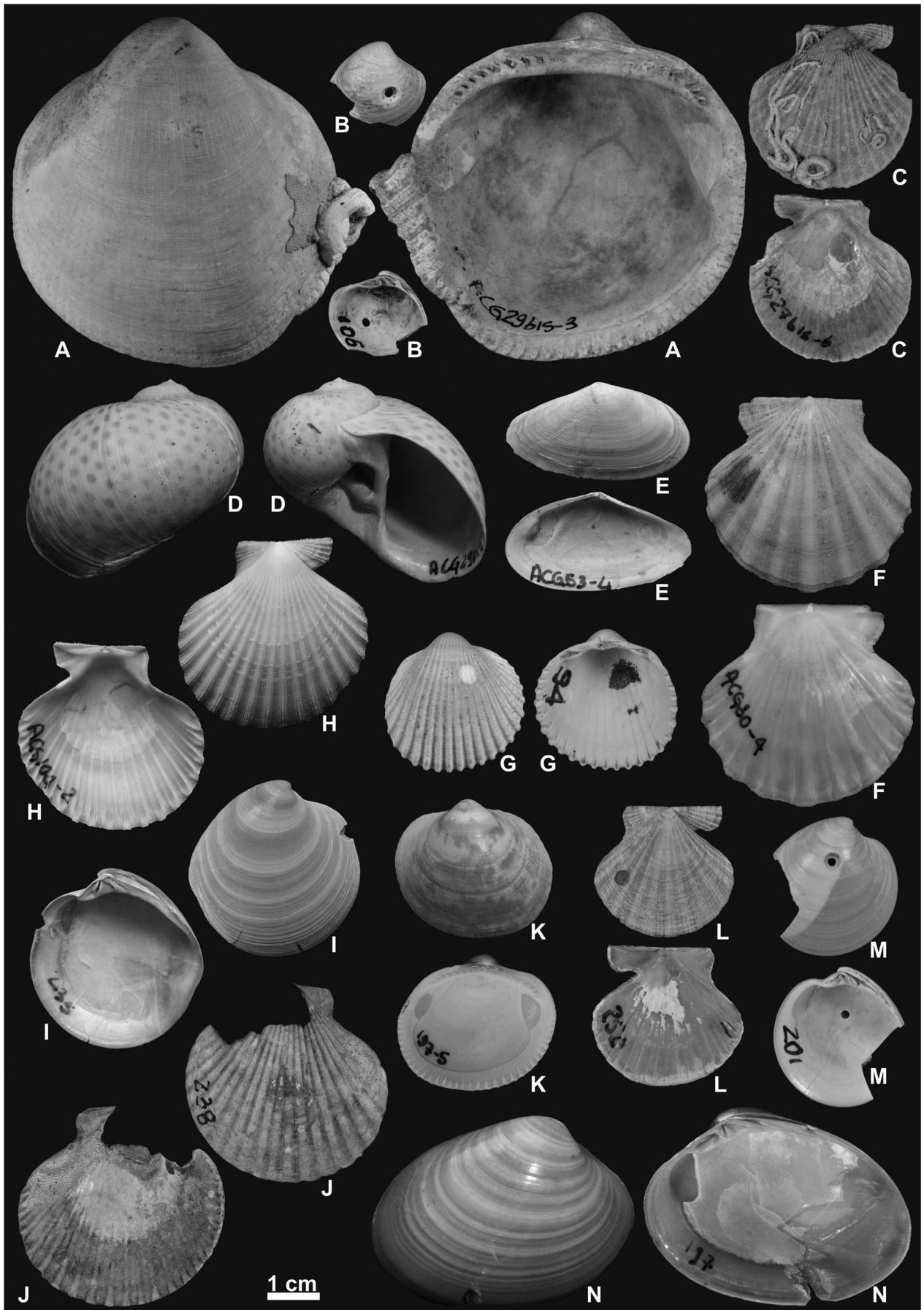
This biofacies occurs in fine-grained massive silts and clays (Facies L; 146.55–167.90 m, 196–207 m). Semi-infaunal/infaunal taxa living in muddy to silty lithologies are dominant. *V. nux* is the most abundant species in this interval, together with *Turritella tricarinata pliorecens*, *Glossus humanus*, *Aporrhais pespelecani*, *Acanthocardia paucicostata*, and *Saccella commutata*, all showing an excellent preservation (Fig. 8B, H; A2 and Table A1 in the Supplementary Information A2 and Supplementary Table A1).

*Interpretation.* The abundance of *V. nux* suggests a low-energy offshore transition setting that can be compared to the recent VTC biocenosis of the Mediterranean Sea (Pérès and Picard, 1964). According to Taviani et al. (1997) and Dominici (2001), the *Venus nux* assemblage lived at water depths of 20–40 m.

### Biofacies 8

This biofacies (80.30–91.40 m; 101–104.10 m; 122.90–125.50 m; Facies L) comprises well-preserved epifaunal species of mainly muddy/sandy-detritic settings (e.g., *Pecten jacobaeus*, *Aequipecten opercularis*, *Flexopecten flexuosus*, and *Pitar rudis*), occurring together with mud-loving infaunal species (as *V. nux* and *T. tricarinata pliorecens*) where the mud content increases (Supplementary Information A2 and Supplementary Table A1).

*Interpretation.* This biofacies is characterized by many key species (e.g., *P. rudis*, *F. flexuosus*, and *P. jacobaeus*)





belonging nowadays to the recent DC biocenosis (Pérès and Picard, 1964) together with VTC species where the mud content increases, all indicating life or neighborhood assemblages of offshore transition environments.

### Biofacies 9

This biofacies is found in an alternation of fossil rich fine-grained sands/silts and mud barren of fossils (127.95–146.45 m; Facies S and B). The fauna consists of well preserved seminafaunal/infaunal species together with few epifaunal ones; taxa of shallow water muddy sands are abundant (e.g., *G. insubrica*, *C. gallina*, *A. tuberculata*, *E. ensis*, and *Tritia mutabilis*) together with few sandy/muddy-detritic species (*A. opercularis*, *Laevicardium oblongum*, and *P. rudis*; Fig. 6F, 7A, 8G, Supplementary Information A1 and Supplementary Table A1). *Ditrupa* sp. horizons are occasionally retrieved (e.g., ACG95; Supplementary Table A1).

**Interpretation.** This biofacies suggests neighborhood assemblages of shoreface settings, which thanks to the presence of *G. insubrica*, *C. gallina*, *A. tuberculata*, *E. ensis*, and *T. mutabilis* can be compared to SFBC biocenosis of the recent Mediterranean Sea (Pérès and Picard, 1964), although a few DC taxa (e.g., *L. oblongum* and *P. rudis*) are also found. Biofacies 9 is similar to Biofacies 5, although very shallow water taxa have not been identified here. The occasional presence of monotaxic beds of *Ditrupa* sp., usually thriving in turbid waters conditions (Dominici, 2001), suggests unstable and loose substrates.

### Biofacies 10

This biofacies occurs in several sandstones beds of the succession within Facies S and B (54–54.20 m; 92.50–98.30 m; 170–194.10 m; 208.40–210.40 m) and is characterized by containing ecologically mixed and generally poorly preserved taxa (Fig. 8I, K, M, M; Supplementary Information A2 and Supplementary Table A1), often associated with clay chips and vegetal debris; an exception is given by well preserved, articulated specimens of *Pinna* sp. and infaunal echinoids. Seminafaunal/infaunal and epifaunal species of shelf muddy/sandy-detritic settings (e.g., *L. oblongum*, *Timoclea ovata*, *P. rudis*, and *P. jacobaeus*) are associated to

shallower water species (e.g., *A. pulchella*, *C. gallina*, *G. insubrica*, and *S. subtruncata*) and mud loving taxa (e.g., *Nucula placentina*, *T. tricarinata pliorecens*, and *V. nux*).

**Interpretation.** This biofacies, characterized by an ecologically mixed poorly preserved fauna of shoreface to offshore transition settings, represents mainly transported assemblages finally buried in an offshore transition setting as testified by articulated *Pinna* sp. and infaunal echinoids in life position (Fig. 6B); this suggests a high-energy setting, also indicated by the facies analysis (Facies S and B).

### Biofacies 11

This biofacies groups species poorly preserved and ecologically mixed (e.g., *A. tuberculata*, *A. opercularis*, and *V. nux*) found within conglomerate beds (217.20 m; 223.80 m; Facies B; Supplementary Information A2 and Table A1).

**Interpretation.** The high taphonomic degradation along the different ecology of the species recovered reflects transport/reworking in a high-energy, coarse-grained, shallow marine settings.

### Trace Fossils

The samples of the Arda River section have been attributed to 15 ichnofabric classes, that are grouped in four ichnofabric groups based on bioturbation intensity, distribution, and diversity (Table 2). Ichnofabric groups and classes were named according to the dominant feature and traces. Ichnotaxa have been identified at the ichnogenus level and open nomenclature has been used for difficultly identifiable traces. Readers are directed to Supplementary Table A2 for details on ichnotaxa.

#### *Ichnofabric group 1 - low-moderate bioturbation, homogeneous distribution of traces, low diversity*

The ichnofabric classes of group 1 typically present low to moderate bioturbation intensity, homogeneous distribution of traces at the scale of the sampling unit and low diversity of traces:

- (1) Unbioturbated ichnofabric. Unbioturbated conglomerates (Facies GmE, Gp);

**Figure 8.** Taphonomic conditions of the body fossils; two views are shown for each specimen: external or internal for bivalves, abapertural or apertural for gastropods. A) *Glycymeris inflata*, left valve; note the encrustation made by bryozoans and serpulids (ACG29bis-3, Biofacies 1, Cycle 0); B) *Pitar rudis*, right valve; note the bioerosion hole reaching the internal part of the valve (ACG106, Biofacies 7, Cycle IV); C) *Aequipecten opercularis*, right valve; the valve is encrusted by serpulids only in the external part (ACG27bis-6, Biofacies 1, Cycle 0); D) *Naticarius stercusmuscarum*, showing preserved original color pattern (ACG29bis-20, Biofacies 1, Cycle 0); E) *Peronidia albicans*, right valve; the finer ornamentation and the color pattern are preserved (ACG53-4, Biofacies 4, Cycle I); F) *Flexopecten glaber*, left valve; the finer ornamentation is preserved (ACG80-4, Biofacies 4, Cycle II); G) *Acanthocardia tuberculata*, right valve; note the attempt of a bioeroding organism to perforate the shell (ACG94, Biofacies 9, Cycle IV); H) *Aequipecten opercularis*, right valve; the finer ornamentation is well preserved (ACG104-2, Biofacies 7, Cycle IV); I) *Dosinia lupinus*, right valve; note the original color pattern (ACG235, Biofacies 10, Cycle VI); J) *Aequipecten opercularis*, left valve; the shell is encrusted by bryozoans both in the interior and exterior (ACG238, Biofacies 10, Cycle VI); K) *Glycymeris insubrica*, left valve; the original color pattern is preserved (ACG197-5, Biofacies 10, Cycle V); L) *Flexopecten glaber*, right valve; the bioerosion does not perforate the entire thickness of the shell (ACG250, Biofacies 5, Cycle VII); M) *Dosinia lupinus*, right valve; hole made by bioeroding organisms (ACG201, Biofacies 10, Cycle V); N) *Callista chione*, right valve; note the preservation of the glossy periostracum (ACG197, Biofacies 10, Cycle V).

←

**Table 2.** Ichnofabrics of the Arda River. Ichnotaxa are described in Supplementary Table A2. The degree of bioturbation is quantified by the ichnofabric index (ii) (Bottjer and Droser, 1991). Firm substrates indicate stiffgrounds (Wetzel and Uchman, 1998) and firmgrounds (Fürsich, 1978; Bromley, 1996). Diversity refers to the typical number of distinct burrows per sampling unit. All ichnofabrics indicate oxic settings.

		Data						Interpretation		
Ichnofabric group	Ichnofabric class	Degree of bioturbation (ii)	Characteristic ichnotaxa	Accessory components	Diversity (n)	Facies	Figures	Depositional environment	Major environmental features	Climate
1	Unbioturbated ichnofabric	1	–	–	0	GmE, Gp	–	Fluvial	–	–
	Low bioturbation ichnofabric	1–2	<i>Planolites</i> , <i>Palaeophycus</i> , cryptobioturbation	–	0–1	Sx, St, Sr	–	Foreshore- middle shoreface	Brackish water	–
	<i>Skolithos</i> ichnofabric	2	<i>Skolithos</i>	–	1	Sm	–	Backshore?; Foreshore-upper shoreface	–	–
	<i>Ophiomorpha</i> ichnofabric	2	<i>Ophiomorpha</i>	<i>Macaronichnus</i>	1	Sh	9A–C	Foreshore-shoreface	High energy	Warm
	<i>Macaronichnus</i> ichnofabric	4–5	<i>Macaronichnus</i>	“Lined light filled burrows”, “unlined light filled burrows”	1	Sm	9D–F	Foreshore-shoreface	High energy	Temperate-cold
2	Few sharp burrows – smooth burrows ichnofabric	1–2	<i>Bergaueria</i>	<i>Fugichnia</i>	0–1	HeB	10A–C	Upper shoreface-offshore	Hyperpycnal-influenced, rhythmical development of firm substrates	–
	Sharp burrows – scollicids ichnofabric	2–3	Scollicids ( <i>Scolicia</i> , <i>Bichordites</i> )	<i>Palaeophycus</i> , <i>Planolites</i> ?, <i>Thalassinoides</i> , oblique burrows, <i>Teichnichnus</i> -like, mantle and swirl structures	1–3	HeB	10G and H	Upper shoreface-offshore	Hyperpycnal-influenced, rhythmical development of firm substrates	Warm
	Sharp burrows – smooth burrows ichnofabric	2–3	“sharp-walled burrows”	Mottles, dark-filled <i>Planolites</i> , <i>Scolicia</i> , <i>Schaubcylindrichnus</i> ? (morphotype A), <i>Palaeophycus</i> , <i>Rosselia</i> ?, <i>Teichichnus</i>	1–5	HeB	10D–F	Offshore	Hyperpycnal-influenced, rhythmical development of firm substrates	–
3	<i>Lockeia</i> ichnofabric	2–3	<i>Lockeia</i> , <i>Ophiomorpha</i> , <i>Siphonichnus</i> , <i>Arenicolites</i> , <i>Diplocraterion</i> , <i>Skolithos</i>	“Winding trails”	0–1	CCB	11A and B	Foreshore?	Firm substrates	–
	<i>Thalassinoides</i> ichnofabric	3–5	<i>Thalassinoides</i>	“Y-shaped burrows”, “columnar burrow sets”	1	Sp	11C and D	Shoreface?	High energy	–
	Coarse-fill burrows ichnofabric	4–5	“Coarse-fill burrows”	–	1	Fm	11 E	Submarine canyon?	Firm substrates	–



Table 2. (Continued)

Ichnofabric group	Ichnofabric class	Degree of bioturbation (ii)	Characteristic ichnotaxa	Data			Interpretation			
				Accessory components	Diversity (n)	Facies	Figures	Depositional environment	Major environmental features	Climate
4	Scollicids ichnofabric	4–5	Scollicids ( <i>Scolicia</i> , <i>Bichordites</i> )	–	1–3	Sm, Fm	12A–C	Lower shoreface -offshore	Hyperpycnal-influenced?	Warm
	<i>Palaeophycus</i> ichnofabric	5–6	<i>Planolites</i> , <i>Palaeophycus</i> , <i>Schaubcylindrichnus</i> ? (morphotype A), <i>Scolicia</i> , <i>Rossetia</i> ?, <i>Teichichnus</i> (morphotype A).	–	3	Sm, Fm	12D–F	Offshore	–	–
	High bioturbation ichnofabric	5–6	Dark-filled <i>Planolites</i> , <i>Schaubcylindrichnus</i> ? (morphotype A), <i>Palaeophycus</i> , <i>Teichichnus</i> (morphotype B), <i>Asterosoma</i> .	Bioerosion traces ( <i>Oichnus</i> , <i>Entobia</i> ?), “shell filled burrows”	0–3	Fm	12G–L	Offshore	–	–

- (2) Low bioturbation ichnofabric. Unbioturbated or sparsely bioturbated (ii 1-2 *Palaeophycus*. Cryptobioturbation locally present;
- (3) *Skolithos* ichnofabric. *Skolithos* occurring in massive sands (Facies Sm);
- (4) *Ophiomorpha* ichnofabric (Fig. 9A–C). *Ophiomorpha* preserved as full-reliefs in planar- or cross-laminated sands (Facies Sh);
- (5) *Macaronichnus* ichnofabric (Fig. 9D–F). *Macaronichnus* preserved in faintly laminated sands with rare shell debris (Facies Sm).

*Interpretation.* The low to moderate bioturbation intensity is interpreted as the result of a stress factor that prevented total bioturbation of the sediment (Bromley, 1996; Taylor et al., 2003). The homogeneous distribution of traces indicates that the stress factors were persistent, at least at the scale of the observation unit (Gingras et al., 2011). Specifically, the ichnofabric classes are interpreted as follows:

- (1) Unbioturbated ichnofabric. The lack of bioturbation suggests the original lack of endobenthic activity or the non-preservation of biogenic structures (Bromley, 1996). Because this ichnofabric is characterized by bed load related facies, it is likely that physical stress, represented by high hydrodynamics and shifting substrates, prevented endobenthic colonization of these units.
- (2) Low bioturbation ichnofabric. This ichnofabric reflects the work of trophic generalists (the producers of *Planolites* and *Palaeophycus*; see Gingras et al., 2011). Brackish setting is suggested by low ichnodiversity, simple structures produced by trophic generalists, monospecific associations, and small size (Pemberton et al., 2001; Buatois et al., 2005; Hauck et al., 2009; Buatois and Mángano, 2011). These features are consistent with a foreshore to middle shoreface environment.
- (3) *Skolithos* ichnofabric. Based on the distribution of both animal and plant *Skolithos* (Bromley, 1996; Gregory et al., 2006; Knaust, 2017), this ichnofabric is interpreted to reflect marine (foreshore to upper shoreface) or, at least, marine-influenced (backshore) settings. A more precise environmental interpretation of this ichnofabric is difficult, also because plant ichnology is an understudied field (Baucon et al., 2012).
- (4) *Ophiomorpha* ichnofabric. This ichnofabric represents the work of a deep-tier community of trophic generalists (the producers of *Ophiomorpha*). The constructional lining of *Ophiomorpha* is a strategy to cope with high-energy and shifting substrates (Frey et al., 1978; Coelho and Rodrigues, 2001; Pemberton et al., 2001; Taylor et al., 2003; Buatois and Mángano, 2011; Gingras et al., 2011). These features are consistent with a high-energy foreshore to shoreface environments (see Pemberton et al., 2001; Baucon et al., 2014; Leaman et al., 2015). Based on the paleoclimatic significance of

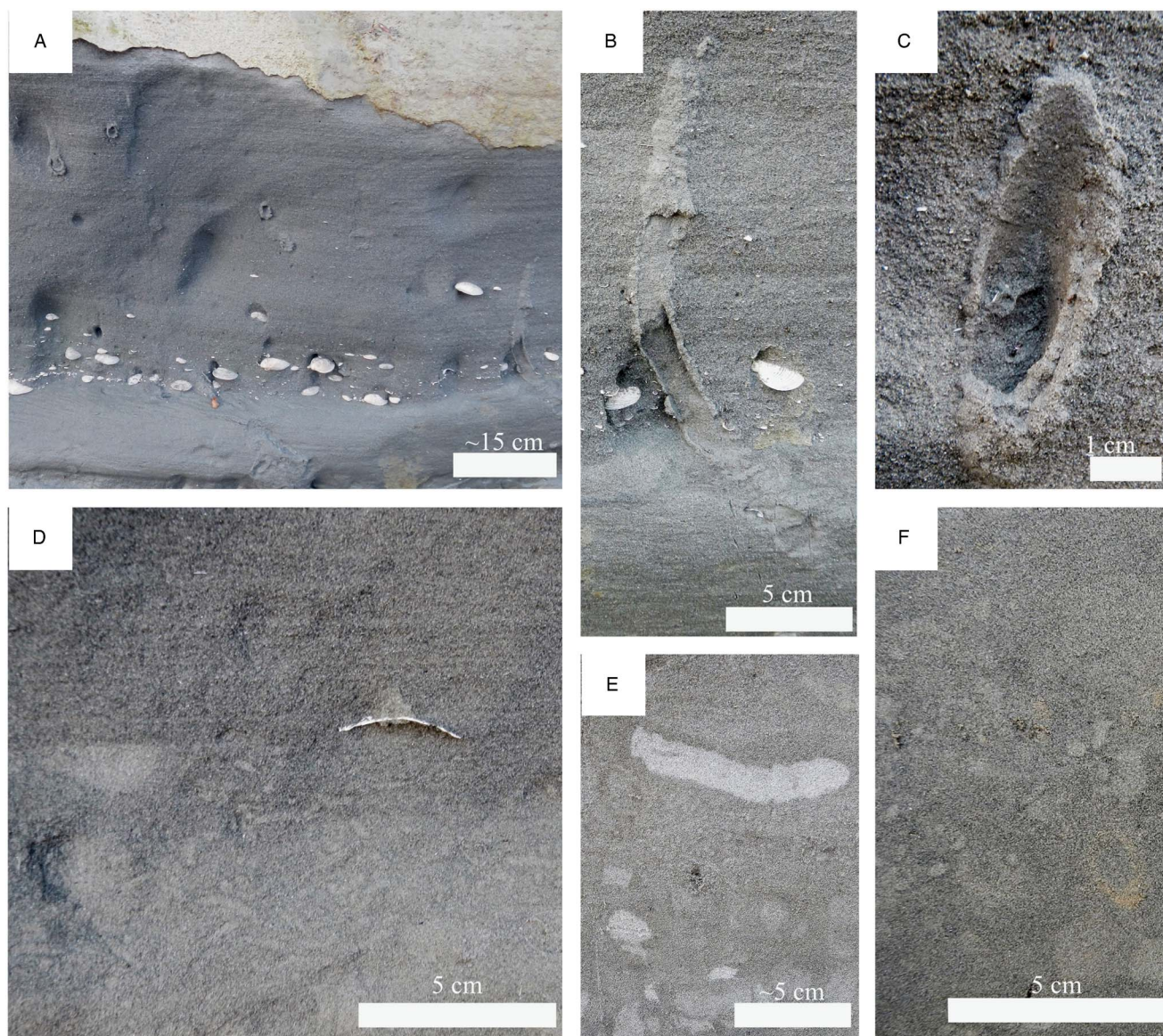


**Figure 9.** (color online) Ichnofabric group 1. (A) *Ophiomorpha* ichnofabric. (B) Close-up of A, showing a specimen of *Ophiomorpha*, parallel lamination, and concave-up shells. (C) *Ophiomorpha* with a robust constructional lining, indicating high-energy conditions. (D) *Macaronichnus* ichnofabric. (E) *Macaronichnus* ichnofabric cross-cut by “lined light filled burrows” (*Ophiomorpha*?). (F) Intensely bioturbated *Macaronichnus* ichnofabric with a significant contribution from other undetermined ichnotaxa.

*Ophiomorpha* (Goldring et al., 2004, 2007), this ichnofabric is regarded as an indicator of warm water.

- (5) *Macaronichnus* ichnofabric. This ichnofabric represents the work of a deep-tier community of selective deposit feeders, well-adapted to soft substrates with very high hydrodynamics at the water-sediment interface. These environmental parameters are compatible to foreshores and shorefaces, as also suggested by the environmental preferences of *Macaronichnus* (high-energy foreshores and shallow shorefaces: Clifton and Thompson, 1978; Pemberton et al., 2001; Savrda and Uddin, 2005; Seike et al., 2011; Pearson et al., 2013). *Macaronichnus* has been proposed as an indicator of temperate to cold waters (Quiroz et al., 2010).

#### *Ichnofabric group 2 - low-moderate bioturbation, heterogeneous distribution of traces, moderate diversity*

The ichnofabric classes of group 2 are characterized by regular heterogeneous distribution of traces. Traces are preserved in heterolithic facies (Fig. 10A) consisting of alternating sand and mud layers (Facies HeB). Mud layers commonly present biogenic structures with poorly defined wall (e.g., *Planolites* and mantle and swirl structures; homogeneous suite; Fig. 10B) and “sharp walled burrows” (sharp burrows suite; Fig. 10C–E). Sand layers are typically bioturbated by lined burrows (e.g., morphotype A of *Schaubcylindrichnus*?; Fig. 9F) and/or smooth-walled traces (e.g., *Scolicia*; Fig. 10G–H). This ichnofabric group comprises three ichnofabric classes,



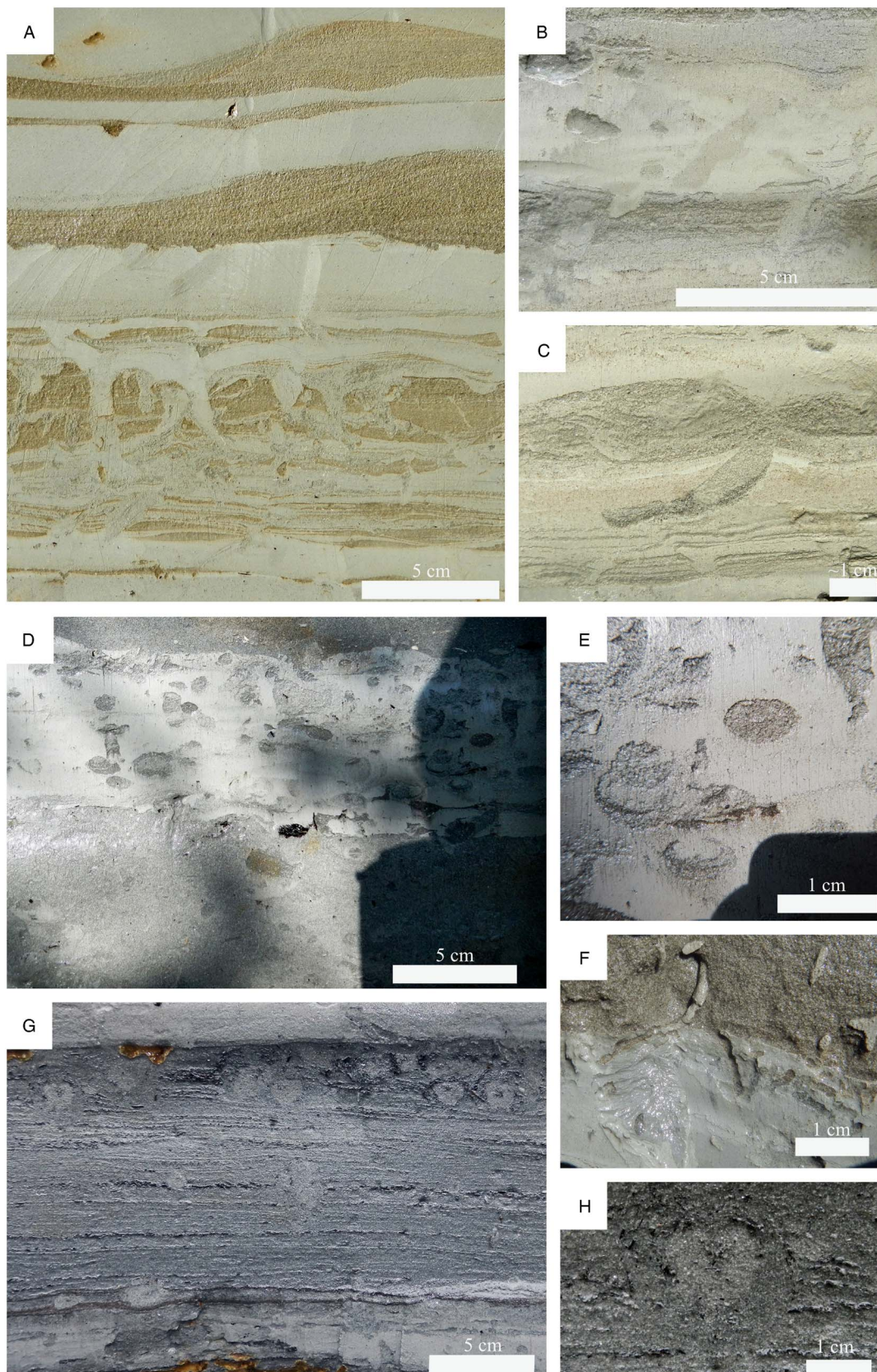


**Figure 10.** (color online) Ichnofabric group 2. (A) Few sharp burrows-smooth burrows ichnofabric. (B) Homogeneous suite represented by biogenic structures with poorly defined walls bioturbating a mud layer. (C) Sharp burrows suite represented by a sharp-walled trace that bioturbated a mud layer. (D) Sharp burrows-smooth burrows ichnofabric. (E) Close-up of D showing several “sharp-walled traces”. (F) *Schaubcylindrichnus?* (morphotype A). (G) Scolicid-sharp burrows ichnofabric. (H) Close-up of G, showing a scolicid and abundant vegetal debris.



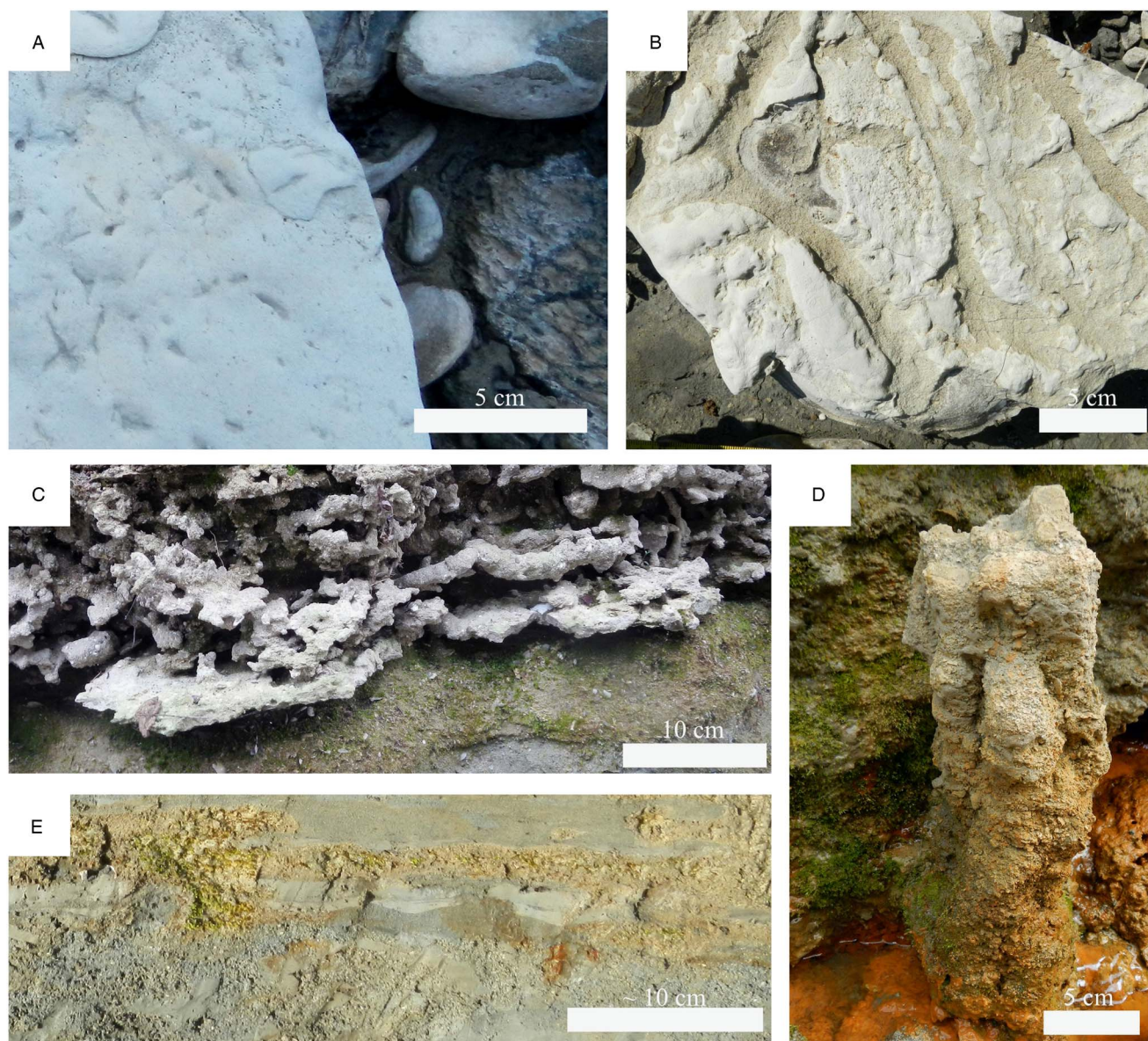


**Figure 11.** (color online) Ichnofabric group 3. (A) *Lockeia* ichnofabric represented by numerous specimens of *Lockeia*; bedding plane view. (B) *Ophiomorpha* preserved in cemented layers. (C) *Thalassinoides* ichnofabric dominated by horizontal burrows filled by bioclastic sands. (D) “Columnar burrow set”. (E) Coarse-fill burrows ichnofabric overlain by sand-mud couplets pertaining to the ichnofabric group 2.

distinguished on the basis of the paucity of “sharp walled burrows” (few sharp burrows, smooth burrows ichnofabric), the dominance of scoloids (sharp burrows, scoloids ichnofabric), and the abundance of “sharp walled burrows” (sharp burrows, smooth burrows ichnofabric).

**Interpretation.** The regular heterogeneous distribution of trace fossils indicates regular variability in the physicochemical conditions and iterative colonization events (Gingras et al., 2011). Based on the hypothesis that burrow boundaries store information about the sediment consistency (Uchman and Wetzel, 2011), these events are interpreted as follows:

(1) Colonization of soupground to softground mud. Traces of the homogeneous suite represent the work of organisms

“swimming” in soupgrounds (mantle and swirl traces) or deposit-feeding in firmer substrates (*Planolites*; Lobza and Schieber, 1999). Settling of hypopycnal plumes or lofting of hyperpycnal flows are interpreted to be the major depositional processes because of sedimentological evidence and the ichnological similarity with other hyperpycnites (Bhattacharya and MacEachern, 2009);

- (2) Dewatering and colonization of firmground mud. The unlined, passively filled burrows of the sharp burrows suite suggest that the sediment became firm enough to avoid collapse of unlined burrows (see Fürsich, 1978; Bromley, 1996; Uchman and Wetzel, 2011);
- (3) Erosion and event deposition. The passive fill of the sharp burrows suite suggests that, after colonization of firmground muds, an abrupt depositional event brought



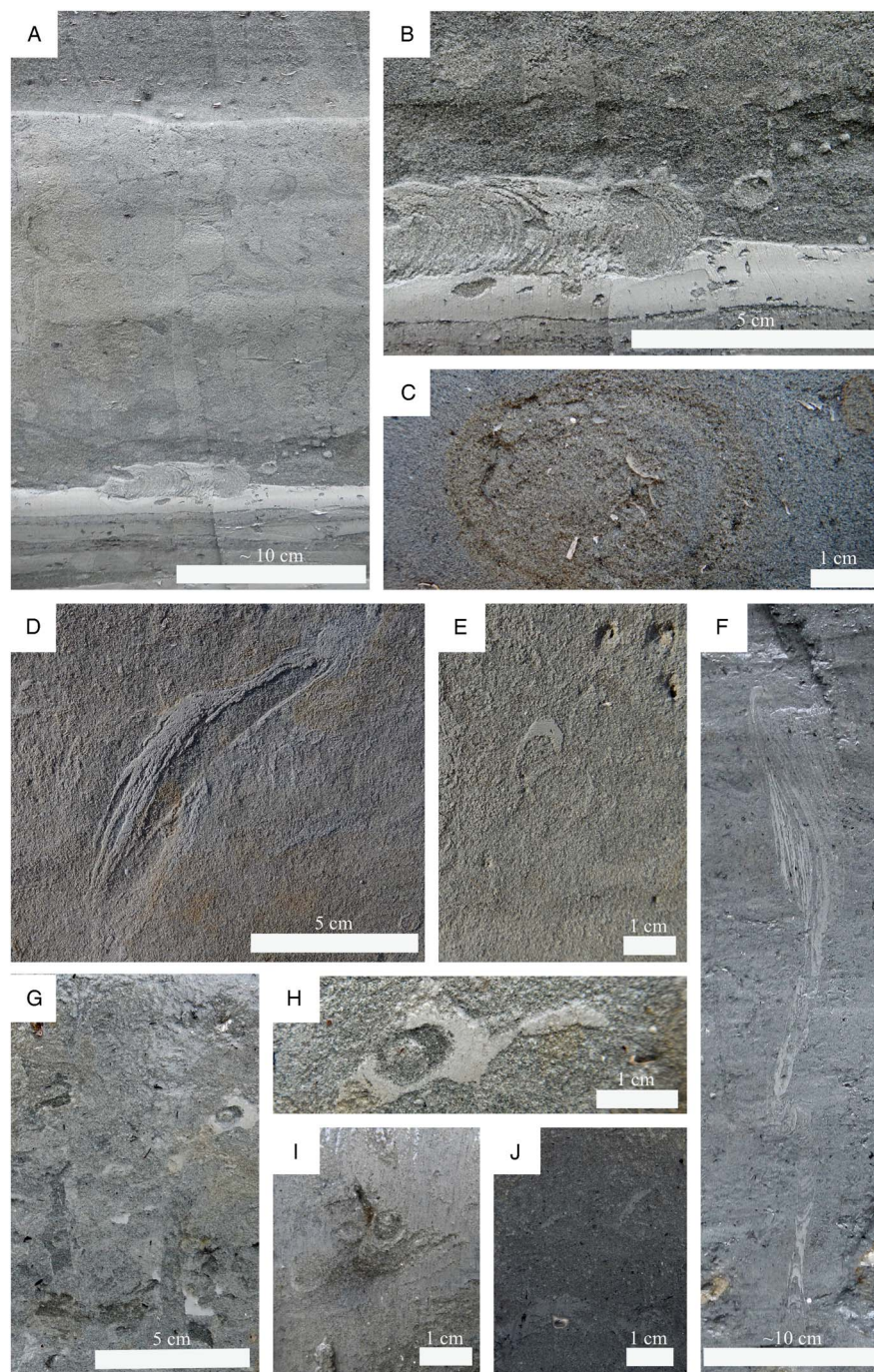


**Figure 12.** (color online) (A) Scolicids ichnofabric overlying the sand/mud couplets typical of ichnofabric group 2. (B) Close-up of A, showing a specimen of *Scolicia* reworking a mud layer. *Palaeophycus* and *Planolites* are present in the sand layer, whereas “sharp-walled traces” bioturbates the mud layer. (C) Scolicid. (D) *Palaeophycus* ichnofabric with a large specimen of *Teichichnus* (morphotype A) and *Palaeophycus*. (E) *Palaeophycus*. (F) *Rosselia*? (G) High bioturbation ichnofabric. (H) Close-up of G, showing a probable specimen of *Asterosoma*. (I) High bioturbation ichnofabric with a distinct *Teichichnus* (morphotype B). (L) High bioturbation ichnofabric with distinct lined vertical burrows (*Schaubcylindrichnus*?)

sand to the seafloor. Hyperpycnal flow is interpreted to be the major depositional process (see Bhattacharya and MacEachern, 2009).

- (4) Colonization of looseground sand. The smooth burrows suite represents the community that colonized sand brought to the seafloor by event deposits (“post-depositional suite”; Książkiewicz, 1954; Seilacher, 1962; Uchman

and Wetzel, 2011). Lining indicates that the substrate was soft and unconsolidated (Bromley, 1996).

For these reasons, the ichnofabric classes of this group are interpreted to reflect bioturbation of muddy seafloors during low-energy conditions and colonization of sandy event (hyperpycnal) deposits. Based on bioturbation intensity,

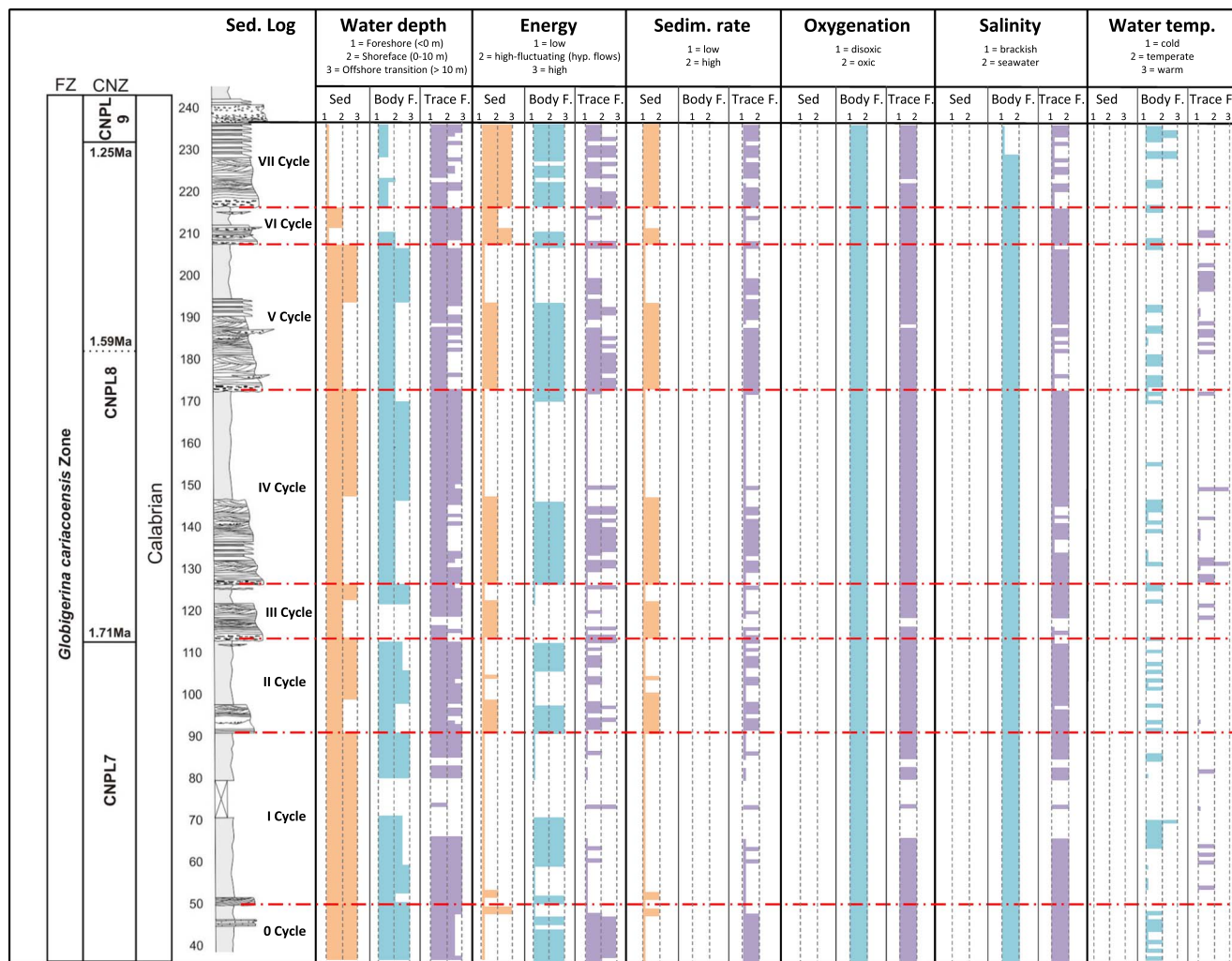


**Figure 13.** (color online) Environmental evolution of the Arda Section. A simplified stratigraphic log (sed. log) with the age of the section, based on calcareous nanofossil (CNZ) and foraminifera (FZ) biostratigraphy, is illustrated (Crippa et al., 2016). For each tool used (Sed, sedimentology; Body, body fossils; Trace, trace fossils) it was analyzed: Water depth: 1, foreshore (region between high tide water level and the low tide water level); 2, shoreface (low tide water level-fair weather wave base); 3, offshore transition and deeper (wave base-shelf edge break; Nichols, 2009). In the modern Adriatic Sea, these regions are respectively at depths of <0 m, 0–10 m, >10 m. Energy: 1, low (nutrients in deposition); 2, high and fluctuating (hyperpycnal flows); 3, high (nutrients in suspension). Sedimentation rate: 1, low; 2, high. Oxygenation: 1, disoxic (2–0.2 ml O<sub>2</sub>/l H<sub>2</sub>O); 2, oxic (8.0–2.0 ml O<sub>2</sub>/l H<sub>2</sub>O; Tyson and Pearson, 1991; Buatois and Mangano, 2011, p.104). Salinity: 1, brackish (0.5–30‰); 2, seawater (30–40‰; Buatois and Mangano, 2011, p. 107). Water temperature: 1, cold; 2, temperate; 3, warm. For body fossils, water temperature was based on oxygen isotope composition of bivalve shells, considering cold >2.5‰; temperate, 0–2.5‰; warm, <0 ‰ (data from Crippa et al., 2016). For trace fossils, climate is defined as following: cold (climate at modern arctic to temperate latitudes), temperate (climate at modern temperate to tropical and subtropical latitudes), and warm (climate at modern tropical and subtropical latitudes). Arctic latitudes are between 66° and 90°, temperate latitudes are between 35° and 66°, tropical and subtropical latitudes are between 0° and 35° (Goldring et al., 2004, 2007).

ichnodiversity, and tiering complexity, the ichnofabric classes of this group are interpreted to reflect a stress gradient, including persistently stressed marine environments (few sharp burrows, smooth burrows ichnofabric), temporarily stressed environments (sharp burrows, scollicids ichnofabric) and stable environments (sharp burrows, smooth burrows ichnofabric). Based on the paleoclimatic significance of *Scolicia* (Goldring et al., 2004, 2007), the sharp burrows-scollicids ichnofabric is interpreted to represent temperate to warm waters. It should be also noted that *Scolicia* is associated with normal marine salinity (Buatois and Mángano, 2011), well-oxygenated porewaters (Löwemark et al., 2006; de Gibert and Goldring, 2008;

Uchman and Wetzel, 2011), restricted competition by organisms of deeper-burrowing tiers (Fu and Werner, 2000), at times being correlated with bottom currents and high sedimentation rates (Fu and Werner, 2000; Löwemark et al., 2006; Wetzel et al., 2011).

*Ichnofabric group 3 - moderate-high bioturbation, homogeneous distribution of traces, low diversity*

Ichnofabric group 3 includes a very heterogeneous set of ichnofabric classes with sharp-walled traces and/or passively filled burrows:



- (1) *Lockeia* ichnofabric (Fig. 11A and B). Cemented carbonatic beds (Facies CCB) with no distinct burrows, or predominantly monogeneric (e.g., *Lockeia*, *Ophiomorpha*, and *Diplocraterion*) assemblages.
- (2) *Thalassinoides* ichnofabric (Fig. 11 C, D). Horizontal, *Thalassinoides* bioturbating, plurimetrical layers of bioclastic sands (Facies Sp). “Y-shaped burrows” and bioerosion structures on shells (e.g., *Entobia*) are also present.
- (3) Coarse-fill burrows ichnofabric (Fig. 11 E). Irregular mottles and circular sharp-walled burrows (*Thalassinoides*?) filled with coarse-grained sand or fine-grained conglomerate.

**Interpretation.** Low diversity and homogeneous distribution of traces suggest persistently stressed conditions or preservation of elite trace fossils by upward migration of deep tiers (Bromley, 1996):

- (1) *Lockeia* ichnofabric. Cementation is a post-colonization feature for the *Ophiomorpha*-dominated assemblages because a loose substrate is required by its tracemakers to manipulate the characteristic pellets of the burrow lining. Other assemblages show some of the characteristics of the substrate-controlled *Glossifungites* ichnofacies (i.e., presence of sharp-walled, unlined dwelling burrows of suspension feeders; dominance of robust, vertical to subvertical, simple, and spreite U-shaped burrows; low ichnodiversity; and high abundance; Buatois and Mángano, 2011). They could represent substrates that became stiff before the colonization by shallow-tier, suspension-feeding organisms. Presence of food in suspension and lack of deep-tier deposit feeders suggests an energetic environment, possibly a high-energy foreshore.
- (2) *Thalassinoides* ichnofabric. This ichnofabric occurs in plurimetrical units bioturbated by *Thalassinoides*, implying that it results from the upward migration of a deep tier. This feature and the passive bioclastic fill suggest that this ichnofabric is the result of repeated cycles of colonization, passive infilling, and deposition. The tubular tempestite model, consisting of the repetitive excavation and storm infilling of burrow networks, could explain this pattern (Tedesco and Wanless, 1991).
- (3) Coarse-fill burrows ichnofabric. Sharp walls and passive fill indicate that biogenic structures have been emplaced in firmground muds and maintained as open burrows (MacEachern et al., 2007, 2012; Buatois and Mángano, 2011). Because the burrow fill differs from surrounding and overlying sediments, this ichnofabric class represents a trace-fossil omission suite that preserves a high-energy event that would otherwise have passed unnoticed (see MacEachern et al., 2012). These features are consistent with an environment dominated by sediment bypass, such as the margins of a submarine canyon, that is a typical depositional setting of the *Glossifungites* ichnofacies (Buatois and Mángano, 2011).

#### *Ichnofabric group 4 - high bioturbation, homogeneous distribution of traces, moderate to high diversity*

The ichnofabric classes of group 4 are typically characterized by intense bioturbation:

- (1) Scolicids ichnofabric (Fig. 12A–C). Scolicids (*Scolicia*, *Bichordites*) bioturbating sands (Facies Sm), silts and sandy muds (Facies Fm);
- (2) *Palaeophycus* ichnofabric (Fig. 12D–F). Numerous distinct burrows (e.g., *Planolites*, *Palaeophycus*, and *Schaubcylindrichnus* – morphotype A) bioturbating sands, silts, and sandy muds (Facies Sm, Fm);
- (3) High bioturbation ichnofabric (Fig. 12G–L). Homogeneous or mottled muds and silts (Facies Fm). Distinct burrows are not always present.

**Interpretation.** High bioturbation intensity and homogeneous bioturbation are interpreted to reflect slow sedimentation, stable, well oxygenated physicochemical conditions (Taylor et al., 2003; Gingras et al., 2011; Uchman and Wetzel, 2011). The ichnofabric classes of this group have been interpreted as follows:

- (1) Scolicids ichnofabric. The abundance in scolicids suggests oxic porewater with normal marine salinities (de Gibert and Goldring, 2008; Buatois and Mángano, 2011); the possible influence of bottom currents (Löwemark et al., 2006; Wetzel et al., 2011); restricted competition by organisms of deeper burrowing tiers (Fu and Werner, 2000); and a good quantity and quality of food (Wetzel, 2010). These environmental features are consistent with an upper shoreface to offshore depositional setting.
- (2) *Palaeophycus* ichnofabric. This ichnofabric class presents similar features with respect to the previously discussed ichnofabric class, but the higher bioturbation intensity and diversity suggest a less-stressed environment. This scenario suggests an offshore depositional environment influenced by hyperpycnal flows.
- (3) High bioturbation ichnofabric. With respect to the other ichnofabrics of the same group, this ichnofabric presents the highest bioturbation intensity, probably indicating higher bioturbation rates, lower sedimentation rates, and a higher availability of food (see Wetzel and Uchman, 1998). These features are interpreted to represent an oxic offshore environment.

## DISCUSSION

### Paleoenvironment of the Arda section

In this section, the seven fining-upward cycles (Fig. 2) have been interpreted in terms of paleoenvironments, integrating the results of sedimentology, body fossil paleontology, and ichnology (Fig. 13).

#### *Cycle 0*

Cycle 0 does not constitute a full cycle, as it lacks the complete facies sequence characterizing Cycles I–VII (see Facies

Association, above). The presence of brachiopods, corals, and echinoids (Biofacies 3; 45.65–46.05 m) as well as the prevalence of high-bioturbation ichnofabric in this cycle would suggest an offshore transition environment characterized by low hydrodynamic energy and low sedimentation rate. Oscillations to high-energy foreshore to shoreface settings with high sedimentation rate do also occur, however, as testified by the presence of rheophilous mollusks in Biofacies 1 (37.05–43.25 m). In addition, the presence (45.20–46.60 m) of a characteristic body of cemented biocalcarene with abundant burrows (*Thalassinoides* ichnofabric) is noteworthy. Different physical conditions can be assumed for its formation, such as reduced fine-grained terrigenous input or strong bottom reworking by currents. The upward reduction of winnowing events restores the initial low-energy conditions characterized by deposition of finer-grained sediments. Here, body fossils show, besides a diagenetic dissolution of aragonitic shells, a high degree of degradation (Biofacies 2; 44.90 m, 47.35–49 m), suggesting a high-energy setting winnowed by currents. In this cycle, oxygen isotope values of bivalve shells (Crippa et al., 2016) point to temperate-cold conditions, related to a mid-shelf environment (depth = ~50 m).

### Cycle I

Cycle I is interpreted to reflect environmental conditions similar to those of the previous cycle, i.e., prevailing offshore transition conditions. Specifically, with the exception of a thin sandstone bed in the basal part, most of Cycle I is represented by monotonous, fine-grained to laminated siltstones (Facies L) deposited by suspension settling from decelerating hyperpycnal flows. Body and trace fossils record a change in the environment; the lower part of the cycle accounts for lower shoreface to offshore transition settings (Biofacies 2 [56.35–58.35 m] and high-bioturbation ichnofabric), whereas the middle part records a temporary shift to shallower and higher-energy foreshore to shoreface settings (Biofacies 4 [59–70.02 m] and presence of the *Macaronichnus* and scollicids ichnofabrics). The topmost part testifies to a return to a deeper water setting (Biofacies 8 [80.30–91.40 m] and high-bioturbation ichnofabric). Although only a few paleotemperature data are available from body fossils of this cycle, these suggest a temperate-cold water environment. Such interpretation is consistent with the presence of *Macaronichnus*, a typical temperate- to cold-water indicator (Quiroz et al., 2010), and *Scollicia*, which, though not exclusive, is common in temperate waters (Goldring et al., 2004, 2007).

### Cycle II

Cycle II mainly documents offshore transition environments recording a cooling event. The basal part of the cycle documents a shoreface environment characterized by high to high-fluctuating energy and high sedimentation rate. This cycle includes coarse-grained deposits related to shear/drag forces exerted by the overpassing long-lived turbulent (hyperpycnal)

flow over coarse-grained materials lying on the flow bottom. High-density flows triggered by river floods can mix and deposit skeletal remains from different shallow-water communities. The poor preservation of body fossils in Biofacies 10 (92.50–98.30 m), the abrupt changes in ichnofabric, the presence of mud clasts and of reworked vegetal debris, besides field observations, all indicate the presence in this interval (91.40–98 m) of a channel cutting obliquely (south-southwest to north-northeast) across the main succession and discharging fresh water and sediments. Aside from this interval, sedimentology and trace fossils document offshore transition environments, whereas body fossils record a shallowing upward trend, passing from an offshore transition environment characterized by low-energy and low sedimentation rate (Biofacies 8; 101–104.10 m) to a shoreface setting with higher energy (Biofacies 4; 106.50–111.60 m). From a paleoclimatic point of view, the first occurrence of the “northern guest” *Arctica islandica* (103.70 m) and the abundant presence of *Macaronichnus* (94 m) mark the beginning of a climatic cooling in the area, which is further supported by bivalve shell oxygen isotope composition (Crippa et al., 2016).

### Cycles III–VI

Cycles III to VI show a more regular organization: each cycle records a deepening upward trend (from foreshore-shoreface to offshore transition settings) and a parallel decrease in hydrodynamic energy and sedimentation rate. Each cycle frequently has an erosive base and starts with conglomerates or rip-up mud clasts (Facies B), followed above by either massive or stratified sandstones (Facies S). Here, low bioturbation ichnofabric indicates brackish conditions, possibly caused by direct fluvial discharge of fresh water and sediments by hyperpycnal flows. This is also supported by the presence of Biofacies 10 (170–194.10 m; 208.40–210.40 m) in Cycles V and VI; this biofacies contains an ecologically mixed fauna and specimens showing poor preservation, both indicating a high-energy environment affected by high-density flows triggered by river floods that mix skeletal remains from different environments. In Cycles III–VI, transported body fossil assemblages and evidence of density flows become more frequent; this means more river discharge and thus more terrigenous input into the Paleo-Adriatic basin. The increase in the tectonic uplift and erosion of the Apennines after 1.80 Ma (e.g., Amorosi et al., 1996; Bartolini et al., 1996; Argnani et al., 1997, 2003; Dominici, 2001, 2004), the proximity to the coast, and possibly climatic deterioration (e.g., increased precipitation and/or increased ice melting during summer and more ice accumulation during winter) may account for the observed increase of hyperpycnal flows in these cycles. The top of each cycle records fully marine conditions with typical faunal associations/ichnofabrics of low-energy settings (Biofacies 7; 146.55–167.90 m, 196–207 m; high bioturbation ichnofabric), reflecting the normal settling when the flow completely stops or sedimentation in a distal portion of the delta system.



Cycle V is particularly rich in scolicid-dominated ichnofabrics. The sedimentological evidence for hyperpycnal flows may indicate that *Scolicia*-dominated ichnofabrics are a proxy for extrabasinal turbidites, sensu Zavala and Arcuri (2016), such as those deposited by hyperpycnal flows. This hypothesis is plausible, as *Scolicia* is correlated with the abundance of food (Wetzel, 2010) and extrabasinal turbidites are rich in phytodetritus because they originated from the continent (Zavala and Arcuri, 2016). By contrast, intrabasinal turbidites originated within the marine basin and are therefore less rich in phytodetritus (Zavala and Arcuri, 2016). Further case studies are required to test this hypothesis.

Paleoclimatic indicators mainly suggest temperate water, although oxygen isotopes from bivalve shells and evidence from trace fossils (*Macaronichnus*) indicate lower water temperatures in a few levels, confirming the change towards cooler climates, affecting the Paleo-Adriatic after the arrival of the “northern guests.” In Cycle III, trace fossils record high-frequency climate fluctuations; abundant *Ophiomorpha*, an ichnological indicator of warm climate, are present at little stratigraphic distance from *Macaronichnus*-dominated horizons.

### Cycle VII

Cycle VII represents the last marine cycle of the Arda succession before the establishment of a continental environment with freshwater mollusks and vertebrate faunas (Bona and Sala, 2016; Monesi et al., 2016); it documents a foreshore to upper shoreface environment characterized by high hydrodynamic energy and high sedimentation rate, due to discharge by fluvial floods. This cycle is characterized by the dominance of ichnofabrics related to brackish water (low bioturbation ichnofabric, few sharp burrows-smooth burrows ichnofabrics). Increased freshwater input, and thus dilution of salinity, is also indicated by the presence of Biofacies 5 (230.80–237 m), recording the only occurrence of *Glycymeris insubrica*, a species that tolerates salinity variations (e.g., Malatesta, 1974; Lozano Francisco et al., 1993; Raineri, 2007; Crnčević et al., 2013). At the top of the succession, Crippa et al. (2016) observed the presence of abundant brackish-water benthic foraminifera and low oxygen isotope ratios in bivalve shells, indicating salinity reduction due to freshwater river discharge. All this evidence, together with the presence of frequent bed-load deposits (Facies B), indicates a foreshore to upper shoreface environment for this part of the section.

### Regional significance of the Arda section

The Arda sedimentary succession represents a valuable case study, as it offers the rare opportunity to study depositional dynamics through phases of strong natural climate change within a tectonically active setting. The stratigraphic and paleontological investigation presented for the Arda section highlights the importance of integrated studies to disentangle the effects of climate and tectonic processes acting to structure sedimentary successions during the early Pleistocene.

In this respect, the overall regressive trend of the marine part of Arda section, consisting of offshore/prodelta (Cycles 0–II) passing to prodelta/delta front (Cycles III–IV) and to intertidal/coastal (Cycle VII) stacked successions, can be directly related to deformation phases of the local fronts of Apennine mountains; this is represented by the change in the dip of the bedding from 20° in the stratigraphically lower part of the section up to <5° in the upper part. While tectonic and climatic forcings are acting simultaneously, regional studies (e.g., Gunderson et al., 2014) indicate that the early Pleistocene (~1.60–1.10 Ma) structuring of this sector of the northern Apennines has been characterized by unsteady but rapid and intense deformation. This specified interval of time encompasses the entire marine sedimentation in the Arda section (see Geological Setting; Crippa et al., 2016). In addition, overall regressive trends were already documented for few other successions outcropping along the northeastern margin of the Apennines, such as the Enza and Stirone River sections (e.g., Pelosio and Raffi, 1977; Dominici, 2001; Gunderson et al., 2014).

The cyclothem nature of the sedimentary succession retains an expression of climatic changes that occurred during the early Pleistocene and was modulated by the morphology of the basin (see Dominici, 2001). Specifically, cyclic stacking patterns of fan-delta forestepping/backstepping episodes described here were produced primarily by the onset and disappearance of local climatic conditions favoring the development of catastrophic flooding through time (see other geologic examples in Weltje and de Boer, 1993; Mutti et al., 1996). Our results correlate well with regional changes at higher temporal frequencies, recording, besides the Apennine uplift, the same evolutionary history of coeval successions in the Castell’Arquato basin and the Paleo-Adriatic region (e.g., Stirone and Enza River sections; Papani and Pelosio, 1962; Dominici, 2001, 2004; Gunderson et al., 2014). The analyses of the biota and of their traces record not only local but also global climate changes. The occurrence of the “northern guest” bivalve *A. islandica*, of *Macaronichnus* trace fossil, and of the “northern guests” foraminifera *Hyalinea balthica* and *Neogloboquadrina pachyderma* left coiling (Crippa et al., 2016) in the section, testify to climatic deterioration, i.e., cooling, which represents an expression of the climatic changes occurring during the early Pleistocene, leading to the onset and establishment of Middle and Upper Pleistocene continental glaciations.

### The multidisciplinary method: advantages and disadvantages

The methodological significance of this study is to provide a multidisciplinary approach to paleoenvironmental reconstructions. Ecosystem evolution is affected by many different factors; instead of just looking at one factor, we followed an integrated approach for the understanding of past environments, integrating three different tools (sedimentology and body and trace fossil paleontology). The practical application of a multidisciplinary approach in paleoenvironmental

reconstructions revealed some methodological advantages and disadvantages. One of the main advantages in applying this method is the possibility to investigate the ecosystems in detail from different points of view, obtaining a more complete and reliable picture of past environments. The use of a single tool, besides giving a one-sided perspective, may be affected by biases specific to the tool itself, which can be avoided or compensated for when using two or more tools. In employing different tools, however, data may also disagree. Disagreements are generally due to different sampling strategies or to problems intrinsic to the tools themselves, e.g., the lack of continuity in the recorded data along the succession and thus a lower resolution scale of analysis, which does not allow the identification of small variations. In the case of the Arda River section, data from sedimentology and body fossils have shown a lower resolution in the scale of analysis compared to trace fossils. For practical reasons, sedimentology, body fossil paleontology, and ichnology involve different sampling schemes, characterized by different resolutions, which also affect the results of the analysis. In some cases, this has led to possible misinterpretations and disagreements between the different tools used; on the other hand, the higher resolution shown by trace fossils has allowed identification of changes at a finer scale of analysis, highlighting also the smallest environmental variation. Generally, we noted that these three different approaches complement one another quite well and compensate for their respective defects, giving strength and robustness to the obtained results, besides a more complete and exhaustive picture of past ecosystems.

The geological record provides a number of different settings and locations within different time intervals, where this multidisciplinary approach can be applied. Elements required are well-exposed, continuous, and age-constrained sedimentary successions rich in fossils (micro-, macro-, and/or trace fossils) and two (although three or more are preferred) different tools on which to base the paleoenvironmental reconstruction. The use of a multidisciplinary approach would greatly improve the resolution of past environment reconstructions and should be applied more frequently for these purposes, taking advantages of the numerous opportunities that the geological record provides.

## CONCLUSION

The detailed multidisciplinary study presented here (sedimentology and body and trace fossils) has proved to be a powerful tool for resolving paleoenvironmental dynamics recorded in sedimentary succession from collisional margins during time intervals of climate change. The paleoenvironmental evolution of the marine Arda River section has been interpreted taking into account the interplay between tectonics and climatic factors. Based upon sedimentology, body fossils, and trace fossils, it corresponds to a subaqueous extension of a fluvial system, originated in a tectonically active setting during phases of advance of fan deltas affected by high-density flows triggered by river floods, which are an

expression of early Pleistocene climate changes. It documents a fully marine and well-oxygenated environment, bounded at the top by continental conglomerates indicating a major sea-level drop and the establishment of a continental environment; indeed, a general regressive trend is observed through the section, passing from a prodelta (Cycles 0–II) to a delta front (Cycles III–IV) and an intertidal zone (Cycle VII) setting. Lower order transgressive and regressive cycles with shifts from lower foreshore-shoreface to offshore transition environments have been identified, with supposed water depths ranging between 5 and 50 m. The hydrodynamic energy and the sedimentation rate are not constant through the section, but they are influenced by hyperpycnal flows which caused an increase in terrigenous input linked to fluvial floods, whose sediments are mainly supplied by an increase in the Apennine uplift and erosion, especially after 1.80 Ma (e.g., Amorosi et al., 1996; Bartolini et al., 1996; Argnani et al., 1997, 2003; Dominici, 2001, 2004). The regressive trend and the climatic deterioration (i.e., cooling) recorded through the section are an expression of the climatic changes occurring during the early Pleistocene; our results correspond well with other studies of both global and local climatic/tectonic changes, recording the same evolutionary history of coeval successions in the Castell'Arquato basin and the Paleo-Adriatic region.

The lower Pleistocene Arda River marine succession represents only one of the numerous case studies provided by the geological record where a multidisciplinary approach can be applied to interpret past complex ecosystems in the frame of climate change and tectonic activity. A multi-approach analysis based on the integration of sedimentological data and body and trace fossils would greatly improve the resolution of paleoenvironmental reconstructions and should also be extended to other geological sites.

## ACKNOWLEDGMENTS

G. Crippa was supported by 2011 Italian Ministry PRIN Project to E. Erba. A. Baucon was supported by the ROSAE project ([www.rosae-project.org](http://www.rosae-project.org)). We warmly thank the editors, S. Schneider, and an anonymous reviewer for their constructive comments that improved the paper. L. Angiolini and M. Marini are thanked for constructive discussions. M. Marini is also warmly thanked for checking the English manuscript.

## SUPPLEMENTARY MATERIAL

To view supplementary material for this article, please visit <https://doi.org/10.1017/qua.2018.10>

## REFERENCES

- Amorosi, A., Farina, M., Severi, P., Preti, D., Caporale, L., Di Dio, G., 1996. Genetically related alluvial deposits across active fault zones: an example of alluvial fan-terrace correlation from the upper Quaternary of the Southern Po Basin Italy. *Sedimentary Geology* 102, 275–295.



- Argnani, A., Barbacini, G., Bernini, M., Camurri, F., Ghielmi, M., Papani, G., Rizzini, F., Rogledi, S., Torelli, L., 2003. Gravity tectonics driven by Quaternary uplift in the Northern Apennines: insights from the La Spezia-Reggio Emilia geo-transect. *Quaternary International* 101–102, 13–26.
- Argnani, A., Bernini, M., Di Dio, G.M., Papani, G., Rogledi, S., 1997. Stratigraphic record of crustal-scale tectonics in the Quaternary of the Northern Apennines (Italy). *Il Quaternario* 10, 595–602.
- Artoni, A., Bernini, M., Papani, G., Rizzini, F., Barbacini, G., Rossi, M., Rogledi, S., Ghielmi, M., 2010. Mass-transport deposits in confined wedge-top basins: surficial processes shaping the messinian orogenic wedge of Northern Apennine of Italy. *Italian journal of geosciences* 129, 101–118.
- Bartolini, C., Caputo, R., Pieri, M., 1996. Pliocene–Quaternary sedimentation in the Northern Apennine Foredeep and related denudation. *Geological Magazine* 133, 255–273.
- Bates, C., 1953. Rational theory of delta formation. *American Association of Petroleum Geologists Bulletin* 37, 2119–2162.
- Baucon, A., Bordy, E., Brustur, T., Buatots, L.A., De, C., Duffin, C., Felletti, F., et al., 2012. A History of Ideas in Ichnology. In: Knaust, D., Bromley, R.G. (Eds.), *Trace Fossils as Indicators of Sedimentary Environments*. Developments in Sedimentology 64, Elsevier, Amsterdam, pp. 3–43.
- Baucon, A., Ronchi, A., Felletti, F., Neto de Carvalho, C., 2014. Evolution of Crustaceans at the edge of the end-Permian crisis: ichnonetwork analysis of the fluvial succession of Nurra (Permian-Triassic, Sardinia, Italy). *Palaeogeography, Palaeoclimatology, Palaeoecology* 410, 74–103.
- Bertini, A., 2010. Pliocene to Pleistocene palynoflora and vegetation in Italy: state of the art. *Quaternary International* 225, 5–24.
- Bhattacharya, J.P., MacEachern, J.A., 2009. Hyperpynal rivers and prodeltaic shelves in the Cretaceous Seaway of North America. *Journal of Sedimentary Research* 79, 184–209.
- Bona, F., Sala, B., 2016. Villafranchian-Galerian mammal faunas transition in South- Western Europe. The case of the late early Pleistocene mammal fauna of the Frantoio locality, Arda River (Castell'Arquato, Piacenza, Northern Italy). *Geobios* 49, 329–347.
- Bottjer, D.J., Droser, M.L., 1991. Ichnofabric and basin analysis. *Palaos* 6, 199–205.
- Brenchley, P.J., Harper, D., 1998. *Palaeoecology: Ecosystems, Environments, and Evolution*. Chapman and Hall, London.
- Brett, C.E., Baird, G.C., 1986. Comparative taphonomy: a key to paleoenvironmental interpretation based on fossil preservation. *Palaos* 1, 207–227.
- Bromley, R.G., 1996. *Trace fossils: Biology, Taphonomy and Applications*. 2nd ed. Chapman and Hall, London.
- Browne, G.H., Naish, T.R., 2003. Facies development and sequence architecture of a late Quaternary fluvial-marine transition, Canterbury Plains and shelf, New Zealand: implications for forced regressive deposits. *Sedimentary Geology* 158, 57–86.
- Bruno, L., Amorosi, A., Severi, P., Costagli, B., 2017. Late Quaternary aggradation rates and stratigraphic architecture of the southern Po Plain, Italy. *Basin Research* 29, 234–248.
- Buatots, L.A., Gingras, M.K., MacEachern, J., Mágano, G.M., Zonneveld, H.-P., Pemberton, S.G., Netto, R.G., Martin, A.J., 2005. Colonization of brackish-water systems through time: evidence from the trace-fossil record. *Palaos* 20, 321–347.
- Buatots, L.A., Mágano, M.G., 2011. *Ichnology: Organism-Substrate Interactions in Space and Time*. Cambridge University Press, Cambridge and New York.
- Calabrese, L., Di Dio, G., 2009. Note Illustrative della Carta Geologica d'Italia alla scala 1: 50.000, foglio 180 "Salsomaggiore Terme". Servizio Geologico d'Italia-Regione Emilia Romagna, Roma.
- Carminati, E., Doglioni, C., 2012. Alps vs. Apennines: the paradigm of a tectonically asymmetric Earth. *Earth Science Reviews* 112, 67–96.
- Carruba, S., Casnedi, R., Felletti, F., 2004. From seismic to bed: surface–subsurface correlations within the turbiditic Cellino Formation (central Italy). *Petroleum Geoscience* 10, 131–140.
- Cau, S., Roveri, M., Taviani, M., 2017. Anatomy of biocalcarenic units in the Plio-Pleistocene record of the Northern Apennines (Italy). *Geophysical Research Abstracts* 19, EGU2017-19478.
- Cau, S., Taviani, M., Manzi, V., Roveri, M., 2013. Paleoecological, bio-sedimentological and taphonomic analysis of Plio-Pleistocene biocalcarenic deposits from northern Apennines and Sicily (Italy). *Journal of Mediterranean Earth Sciences Special Issue*, 35–37.
- Ceregato, A., Raffi, S., Scarponi, D., 2007. The circalittoral/bathyal in the Middle Pliocene of Northern Italy: the case of the *Korobkovia oblonga*–*Jupiteria concava* paleocommunity type. *Geobios* 40, 555–572.
- Ciangherotti, A.D., Crispino, P., Esu, D., 1997. Paleoecology of the non-marine molluscs of the Pleistocene Stirone River sequence (Emilia, Northern Italy). *Bollettino della Società Paleontologica Italiana* 36, 303–310.
- Cigala Fulgosi, F., 1976. *Dicerorhinus hemitoechus* (Falconer) del post-Villafranchiano fluvio lacustre del T. Stirone (Salsomaggiore, Parma). *Bollettino della Società Paleontologica Italiana* 15, 59–72.
- Clifton, H.E., Thompson, J.K., 1978. *Macaronichnus segregatis*: a feeding structure of shallow marine polychaetes. *Journal of Sedimentary Petrology* 48, 1293–1302.
- Coelho, V.R., Rodrigues, S. de A., 2001. Trophic behaviour and functional morphology of the feeding appendages of the laomediid shrimp *Axianassa australis* (Crustacea: Decapoda: Thalassinidea). *Journal of the Marine Biological Association of the United Kingdom* 81, 441–454.
- Combourieu-Nebout, N., Bertini, A., Russo-Ermolli, E., Peyron, O., Klotz, S., Montade, V., Fauquette, S., et al., 2015. Climate changes in the central Mediterranean and Italian vegetation dynamics since the Pliocene. *Review of Palaeobotany and Palynology* 218, 127–147.
- Crippa, G., Angiolini, L., Bottini, C., Erba, E., Felletti, F., Frigerio, C., Hennissen, J.A.I., et al., 2016. Seasonality fluctuations recorded in fossil bivalves during the early Pleistocene: Implications for climate change. *Palaeogeography, Palaeoclimatology, Palaeoecology* 446, 234–251.
- Crippa, G., Raineri, G., 2015. The genera *Glycymeris*, *Aequipecten* and *Arctica*, and associated mollusk fauna of the Lower Pleistocene Arda River section (Northern Italy). *Rivista Italiana di Paleontologia e Stratigrafia* 121, 61–101.
- Crnčević, M., Balić, D.E., Pećarević, M., 2013. Reproductive cycle of *Glycymeris nummaria* (Linnaeus, 1758) (Mollusca: Bivalvia) from Mali Ston Bay, Adriatic Sea, Croatia. *Scientia Marina* 77, 293–300.
- de Gibert, J., Goldring, R., 2008. Spatangoid-produced ichnofabrics (Bateig Limestone, Miocene, Spain) and the preservation of spatangoid trace fossils. *Palaeogeography, Palaeoclimatology, Palaeoecology* 270, 299–310.
- Dodd, J.R., Stanton, R.J., 1990. *Paleoecology: Concepts and Applications*. 2nd ed. John Wiley and Sons, New York.
- Dominici, S., 2001. Taphonomy and paleoecology of shallow marine macrofossil assemblages in a collisional setting (late

- Pliocene–early Pleistocene, western Emilia, Italy). *Palaios* 16, 336–353.
- Dominici, S., 2004. Quantitative Taphonomy in Sandstones from an Ancient Fan Delta System (Lower Pleistocene, Western Emilia, Italy). *Palaios* 19, 193–205.
- Felletti, F., Carruba, S., Casnedi, R., 2009. Sustained turbidity currents: evidence from the Pliocene Periadriatic foredeep (Cellino Basin, Central Italy). External Controls on Deep-Water Depositional Systems. *Society for Sedimentary Geology Special Publication* 92, 325–346.
- Frey, R.W., Howard, J.D., Pryor, W.A., 1978. *Ophiomorpha*: its morphologic, taxonomic, and environmental significance. *Palaeogeography, Palaeoclimatology, Palaeoecology* 23, 199–229.
- Fu, S., Werner, F., 2000. Distribution, ecology and taphonomy of the organism trace, *Scolicia*, in northeast Atlantic deep-sea sediments. *Palaeogeography, Palaeoclimatology, Palaeoecology* 156, 289–300.
- Fürsich, F.T., 1978. The influence of faunal condensation and mixing on the preservation of fossil benthic communities. *Lethaia* 11, 243–250.
- Fusco, F., 2010. *Picea* + *Tsuga* pollen record as a mirror of oxygen isotope signal? An insight into the Italian long pollen series from Pliocene to Early Pleistocene. *Quaternary International* 225, 58–74.
- Ghibaudo, G., 1992. Subaqueous sediment gravity flow deposits: practical criteria for their field description and classification. *Sedimentology* 39, 423–454.
- Gingras, M.K., MacEachern, J.A., Dashtgard, S.E., 2011. Process ichnology and the elucidation of physico-chemical stress. *Sedimentary Geology* 237, 115–134.
- Goldring, R., Cadée, G., D’Alessandro, A., de Gibert, J.M., Jenkins, R., Pollard, J.E., 2004. Climatic control of trace fossil distribution in the marine realm. In: McIlroy, D. (Ed.), *The Application of Ichnology to Palaeoenvironmental and Stratigraphic Analysis*. Geological Society of London, Special Publications 228. Geological Society of London, London, pp. 77–92.
- Goldring, R., Cadée, G., Pollard, J.E., 2007. Climatic Control of Marine Trace Fossil Distribution. In: Miller W., III (Ed.), *Trace Fossils: Concepts, Problems, Prospects*. Elsevier, Amsterdam, pp. 159–171.
- Gregory, M.R., Campbell, K.A., Zuraida, R., Martin, A.J., 2006. Plant Traces Resembling *Skolithos*. *Ichnos* 13, 205–216.
- Gunderson, K.L., Pazzaglia, F.J., Picotti, V., Anastasio, D.A., Kodama, K.P., Rittenour, T., Frankel, K.F., et al., 2014. Unraveling tectonic and climatic controls on synorogenic growth strata (Northern Apennines, Italy). *Geological Society of America Bulletin* 126, 532–552.
- Hauck, T.E., Dashtgard, S.E., Pemberton, S.G., Gingras, M.K., 2009. Brackish-water ichnological trends in a micro-tidal barrier island/embayment system, Kouchibouguac National Park, New Brunswick, Canada. *Palaios* 24, 478–496.
- Knaust, D., 2017. Atlas of Trace Fossils in Well Core. Springer, Cham, Switzerland.
- Kowalewski, M., Wittmer, J.M., Dexter, T.A., Amorosi, A., Scarponi, D., 2015. Differential response of marine communities to natural and anthropogenic changes. Proceedings of the Royal Society B 282. <http://dx.doi.org/10.1098/rspb.2014.2990>.
- Książkiewicz, M., 1954. Uwarstwienie frakcyjne i laminowane we fliszu karpaccim (Graded and laminated bedding in the Carpathian Flysch). [In Polish with English summary]. *Rocznik Polskiego Towarzystwa Geologicznego* 22, 399–471.
- Leaman, M., McIlroy, D., Herringshaw, L.G., Boyd, C., Callow, R. H.T., 2015. What does *Ophiomorpha irregulaire* really look like? *Palaeogeography, Palaeoclimatology, Palaeoecology* 439, 38–49.
- Lozba, V., Schieber, J., 1999. Biogenic sedimentary structures produced by worms in soupy, soft muds: observations from the Chattanooga Shale (Upper Devonian) and experiments. *Journal of Sedimentary Research* 69, 1041–1049.
- Löwemark, L., Lin, Y., Chen, H.-F., Yang, T.-N., Beier, C., Werner, F., Lee, C.-Y., Song, S.-R., Kao, S.-J., 2006. Sapropel burn-down and ichnological response to late Quaternary sapropel formation in two ~400 ky records from the eastern Mediterranean Sea. *Palaeogeography, Palaeoclimatology, Palaeoecology* 239, 406–425.
- Lozano Francisco, M.C., Vera Pelaez, J.L., Guerra Merchan, A., 1993. Arcoïda (Mollusca, bivalvia) del Plioceno de la provincia de Málaga, España. *Treballs del Museu de Geologia de Barcelona* 3, 157–188.
- MacEachern, J.A., Bann, K.L., Gingras, M.K., Zonneveld, J.-P., Dashtgard, S., Pemberton, S.G., 2012. The Ichnofacies Paradigm. In: Knaust, D., Bromley, R.G. (Eds.), *Trace Fossils as Indicators of Sedimentary Environments. Developments in Sedimentology* 64, 563–603.
- MacEachern, J.A., Pemberton, S.G., Gingras, M.K., Bann, K.L., 2007. The ichnofacies concept: a fifty-year retrospective. In: Miller W., III (Ed.), *Trace Fossils: Concepts, Problems, Prospects*. Elsevier, Amsterdam, pp. 50–75.
- Malatesta, A., 1974. Malacofauna pliocenica umbra. *Memoria per servire alla descrizione della Carta Geologica d’Italia* 13, 1–490.
- Mancini, M., Moscatelli, M., Stigliano, F., Cavinato, G.P., Marini, M., Pagliaroli, A., Simionato, M., 2013. Fluvial facies and stratigraphic architecture of Middle Pleistocene incised valleys from the subsoil of Rome (Italy). *Journal of Mediterranean Earth Sciences Special Issue*, 89–93.
- Marini, M., Milli, S., Rossi, M., De Tomasi, V., Meda, M., Lisi, N., 2013. Multi-scale characterization of the Pleistocene-Holocene Tiber delta deposits as a depositional analogue for hydrocarbon reservoirs. *Journal of Mediterranean Earth Sciences Special Issue*, 103–109.
- Martinelli, J.C., Soto, L.P., González, J., Rivadeneira, M.M., 2017. Benthic communities under anthropogenic pressure show resilience across the quaternary. *Royal Society Open Science* 4, 170796. DOI:10.1098/rsos.170796.
- Martínez-García, B., Rodríguez-Lázaro, J., Pascual, A., Mendicoa, J., 2015. The “northern guests” and other palaeoclimatic ostracod proxies in the late quaternary of the Basque basin (S bay of Biscay). *Palaeogeography, Palaeoclimatology, Palaeoecology* 419, 100–114.
- Massari, F., Chiocci, F., 2006. Biocalcarene and mixed cool-water prograding bodies of the Mediterranean Pliocene and Pleistocene: architecture, depositional setting and forcing factors. *Geological Society of London Special Publications* 255.1, 95–120.
- McIlroy, D., 2004. The application of ichnology to palaeoenvironmental and stratigraphic analysis. *Geological Society of London Special Publications* 228, 1–2.
- McIlroy, D., 2008. Ichnological analysis: The common ground between ichnofacies workers and ichnofabric analysts. *Palaeogeography, Palaeoclimatology, Palaeoecology* 270, 332–338.
- Milli, S., Mancini, M., Moscatelli, M., Stigliano, F., Marini, M., Cavinato, G.P., 2016. From river to shelf, anatomy of a high-frequency depositional sequence: the Late Pleistocene to Holocene Tiber depositional sequence. *Sedimentology* 63, 1886–1928.



- Monegatti, P., Raffi, S., Roveri, M., Taviani, M., 2001. One day trip in the outcrops of Castell'Arquato Plio–Pleistocene Basin: from the Badlands of Monte Giogo to the Stirone River. *Paleobiogeography and Paleocology 2001 International Conference, Excursion Guidebook*, Università di Parma, Parma, Italy, pp. 26.
- Monesi, E., Muttoni, G., Scardia, G., Felletti, F., Bona, F., Sala, B., Tremolada, F., Francou, C., Raineri, G., 2016. Insights on the opening of the Galerian mammal migration pathway from magnetostratigraphy of the Pleistocene marine–continental transition in the Arda River section (northern Italy). *Quaternary Research* 86, 220–231.
- Mulder, T., Syvitski, J.P.M., Migeon, S., Faugères, J.C., Savoye, B., 2003. Marine hyperpycnal flows: Initiation, behavior and related deposits. A review. *Marine and Petroleum Geology* 20, 861–882.
- Mutti, E., Davoli, G., Tinterri, R., Zavala, C., 1996. The importance of ancient fluvio-deltaic systems dominated by catastrophic flooding in tectonically active basins. *Memorie di Scienze Geologiche* 84, 233–291.
- Mutti, E., Tinterri, R., Benevelli, G., Di Biase, D., Cavanna, G., 2003. Deltaic, mixed and turbidite sedimentation of ancient foreland basins. *Marine and Petroleum Geology* 20, 733–755.
- Mutti, E., Tinterri, R., Di Biase, D., Fava, L., Mavilla, N., Angella, S., Calabrese, L., 2000. Delta-front facies associations of ancient flood-dominated fluvio-deltaic systems. *Revista Societá Geologica de España* 13, 165–190.
- Nichols, G., 2009. *Sedimentology and Stratigraphy*. 2nd ed. Wiley-Balckwell, Chichester.
- Ori, G.G., Roveri, M., Vannoni, F., 1986. Plio-Pleistocene sedimentation in the Apenninic-Adriatic foredeep (Central Adriatic Sea, Italy). *International Association of Sedimentologists Special Publication* 8, 183–198.
- Papani, G., Pelosio, G., 1962. (1963). La serie plio-pleistocenica del Torrente Stirone (Parmense Occidentale). *Bollettino della Societá Geologica Italiana* 81, 293–325.
- Pearson, N.J., Gabriela Mángano, M., Buatois, L.A., Casadío, S., Raising, M.R., 2013. Environmental variability of *Macaronichnus ichnofabrics* in Eocene tidal-embayment deposits of southern Patagonia, Argentina. *Lethaia* 46, 341–354.
- Pelosio, G., Raffi, S., 1977. Preliminary remarks on mollusc assemblages of the Stirone river Pleistocene series (Parma Province, Northern Italy). In: Bowen, D.Q. (Ed.), X INQUA Congress Excursion Guides Vol. X. International Union for Quaternary Research, Birmingham, England, pp. 1–19.
- Pemberton, S.G., Spila, M., Pulham, A.J., Saunders, T., MacEachern, J.A., Robbins, D., Sinclair, I.K., 2001. *Ichnology and Sedimentology of Shallow to Marginal Marine Systems*. Geological Association of Canada, Short Course Notes, Vol. 15. AGMV Marquis, St. John's.
- Pèrès, J.M., Picard, J., 1964. Nouveau manuel de bionomie bentique de la Méditerranée. *Recueil des Travaux de la Station Marine d'Endoume* 31, 1–137.
- Pieri, M., 1983. Three seismic profiles through the Po Plain. In: Bally, A.W. (Ed.), *Seismic Expression of Structural Styles*. American Association of Petroleum Geologists, Studies in Geology Series 15. The American Association of Petroleum Geologists, Tulsa, Oklahoma, pp. 3.4.1/8–3.4.1/26.
- Quiroz, L.I., Buatois, L.A., Mangano, M.G., Jaramillo, C.A., Santiago, N., 2010. Is the trace fossil *Macaronichnus* an indicator of temperate to cold waters? Exploring the paradox of its occurrence in tropical coasts. *Geology* 38, 651–654.
- Raffi, S., 1986. The significance of marine boreal molluscs in the Early Pleistocene faunas of the Mediterranean area. *Palaeogeography, Palaeoclimatology, Palaeoecology* 52, 267–289.
- Raineri, G., 2007. *Riserva Naturale Geologica del Piacenziano: Appunti per un'Escursione*. Parchi e Riserve dell'Emilia-Romagna, Rome, Italy.
- Ricci Lucchi, F., 1986. Oligocene to Recent foreland basins of northern Apennines. In: Allen, P.H., Homewood, P. (Eds.), *Foreland Basins*. International Association of Sedimentologists, Special Publication No. 8, International Association of Sedimentologists, CITY, pp. 105–139.
- Roveri, M., Taviani, M., 2003. Calcarene and sapropel deposition in the Mediterranean Pliocene: shallow-and deep-water record of astronomically driven climatic events. *Terra Nova* 15, 279–286.
- Roveri, M., Visentin, C., Argnani, A., Knezaurek, G., Lottaroli, F., Rossi, M., Taviani, M., Trincardi, F., Vigliotti, L., 1998. The Castell'Arquato Basin: high-resolution sequence stratigraphy and stratal patterns of an uplifting margin in the Apennines foothills (Italy). In: M. Field, S. Berné, A. Colella, C. Nittrouer, F. Trincardi (Eds.), *SEPM–IAS Research Conference (September 15–19, 1998): Strata and Sequences on Shelves and Slopes, Abstract Volume*. SEPM-IAS, Sicily.
- Savrda, C., Uddin, A., 2005. Large *Macaronichnus* and Their Behavioral Implications (Cretaceous Eutaw Formation, Alabama, USA). *Ichnos* 12, 1–9.
- Scarponi, D., Huntley, J.W., Capraro, L., Raffi, S., 2014. Stratigraphic paleoecology of the Valle di Manche section (Crotone Basin, Italy): a candidate GSSP of the Middle Pleistocene. *Palaeogeography, Palaeoclimatology, Palaeoecology* 402, 30–43.
- Scarponi, D., Azzarone, M., Kowalewski, M., Huntley, J.W., 2017a. Surges in trematode prevalence linked to centennial-scale flooding events in the Adriatic. *Nature Scientific Reports* 7, 5732. <http://dx.doi.org/10.1038/s41598-017-05979-6>.
- Scarponi, D., Kusnerik, K., Azzarone, M., Amorosi, A., Bohacs, K., Drexler, T.M., Kowalewski, M., 2017b. Systematic vertical and lateral changes in quality and time resolution of the macrofossil record: insights from Holocene transgressive deposits, Po coastal plain, Italy. *Marine and Petroleum Geology* 87, 128–136.
- Schäfer, W., 1956. Wirkungen der Benthos Organismen auf den jungen Schichtverband. *Senckenbergiana Lethaea* 37, 183–263.
- Seike, K., Yanagishima, S.I., Nara, M., Sasaki, T., 2011. Large *Macaronichnus* in modern shoreface sediments: identification of the producer, the mode of formation, and paleoenvironmental implications. *Palaeogeography, Palaeoclimatology, Palaeoecology* 311, 224–229.
- Seilacher, A., 1962. Paleontological studies on turbidite sedimentation and erosion. *The Journal of Geology* 70, 227–234.
- Suess, E., 1883–1888. *Das Antlitz der Erde*. F. Tempsky (Prague, Czech Republic; Vienna, Austria) and G. Freytag (Leipzig, Germany).
- Taviani, M., Roveri, M., Impiccini, R., Vigliotti, L., 1997. Segnalazione di Quaternario marino nella Val Chero (Appennino Piacentino). *Bollettino della Societá Paleontologica Italiana* 36, 331–338.
- Taylor, A., Goldring, R., Gowland, S., 2003. Analysis and application of ichnofabrics. *Earth-Science Reviews* 60, 227–259.
- Taylor, P.D., Wilson, M.A., 2003. Palaeoecology and evolution of marine hard substrate communities. *Earth-Science Reviews* 62, 1–103.
- Tedesco, L.P., Wanless, H.R., 1991. generation of sedimentary fabrics and facies by repetitive excavation and storm infilling of burrow networks, Holocene of South Florida and Caicos Platform, B.W.I. *Palaaios*, 326–343.

- Tinterri, R., 2007. The Lower Eocene Roda Sandstone (South-Central Pyrenees): an example of a flood-dominated river-delta system in a tectonically controlled basin. *Rivista Italiana di Paleontologia e Stratigrafia* 113, 223–255.
- Tyson, R., Pearson, T.H., 1991. Modern and ancient continental shelf anoxia: an overview. *Geological Society of London Special Publications* 58, 1–24.
- Uchman, A., Wetzel, A., 2011. Deep-sea ichnology: the relationships between depositional environment and endobenthic organisms. In: Huneke, H., Mulder, T. (Eds.), *Deep-Sea Sediments*. Developments in Sedimentology 63, Elsevier, Amsterdam, pp. 517–556.
- von Leesen, G., Beierlein, L., Scarponi, D., Schöne, B.R., Brey, T., 2017. A low seasonality scenario in the Mediterranean Sea during the Calabrian (Early Pleistocene) inferred from fossil *Arctica islandica* shells. *Palaeogeography, Palaeoclimatology, Palaeoecology* 485, 706–714.
- Weltje, G., de Boer, P.L., 1993. Astronomically induced paleoclimatic oscillations reflected in Pliocene turbidite deposits on Corfu (Greece): implications for the interpretation of higher order cyclicity in ancient turbidite systems. *Geology* 21, 307–310.
- Wetzel, A., 2010. Deep-sea ichnology: Observations in modern sediments to interpret fossil counterparts. *Acta Geologica Polonica* 60, 125–138.
- Wetzel, A., Tjallingii, R., Wiesner, M.G., 2011. Bioturbational structures record environmental changes in the upwelling area off Vietnam (South China Sea) for the last 150,000 years. *Palaeogeography, Palaeoclimatology, Palaeoecology* 311, 256–267.
- Wetzel, A., Uchman, A., 1998. Deep-sea benthic food content recorded by ichnofabrics: a conceptual model based on observations from Paleogene Flysch, Carpathians, Poland. *Palaios* 13, 533–546.
- Williams, A., Brunton, C.H.C., Carlson, S.J., Alvarez, F., Ansell, A.D., Baker, P.G., Bassett, M.G., et al., 2000. Linguliformea, Craniiformea and Rhynchonelliformea (part). In: Kaesler, R.L. (Ed.), *Treatise on Invertebrate Paleontology, Part H, Brachiopoda, Revised*. The Geological Society of America and The University of Kansas, Boulder, Colorado and Lawrence, Kansas, Vol. 2, pp. 423; Vol. 33 pp. 424–919.
- Williams, A., Brunton, C.H.C., Carlson, S.J., Alvarez, F., Ansell, A.D., Baker, P.G., Bassett, M.G., et al., 2006. Rhynchonelliformea (part). In: Kaesler, R.L. (Ed.), *Treatise on Invertebrate Paleontology, Part H, Brachiopoda, Revised*. The Geological Society of America and The University of Kansas, Boulder, Colorado and Lawrence, Kansas, Vol. 5, pp. 1689–2320.
- Wittmer, J.M., Dexter, T.A., Scarponi, D., Amorosi, A., Kowalewski, M., 2014. Quantitative bathymetric models for late Quaternary transgressive-regressive cycles of the Po Plain, Italy. *The Journal of Geology* 122, 649–670.
- Wysocka, A., Radwański, A., Górka, M., Bąbel, M., Radwańska, U., Złotnik, M., 2016. The Middle Miocene of the Fore-Carpathian Basin (Poland, Ukraine and Moldova). *Acta Geologica Polonica* 66, 351–401.
- Zavala, C., Arcuri, M., 2016. Intrabasinal and extrabasinal turbidites: origin and distinctive characteristics. *Sedimentary Geology* 337, 36–54.
- Zavala, C., Arcuri, M., Di Meglio, M., Gamero Diaz, H., Contreras, C., 2011. A genetic facies tract for the analysis of sustained hyperpycnal flow deposits. In: Slatt, R.M., Zavala, C. (Eds.), *Sediment Transfer from Shelf to Deep Water: Revisiting the Delivery System*. American Association of Petroleum Geologists *Studies in Geology* 61, 31–35.
- Zavala, C., Ponce, J., Dritanti, D., Arcuri, M., Freije, H., Asensio, M., 2006. Ancient lacustrine hyperpycnites: a depositional model from a case study in the Rayoso Formation (Cretaceous) of west-central Argentina. *Journal of Sedimentary Research* 76, 41–59.